UNIVERSITA' DEGLI STUDI DI VERONA

DEPARTMENT OF

Diagnostic and Public Health

GRADUATE SCHOOL OF

Natural Sciences and Engineering

DOCTORAL PROGRAM IN

Nanoscience and Advanced Technologies

Cycle / year (1° year of attendance) 32°/2016

TITLE OF THE DOCTORAL THESIS

Interferon Regulatory Factor 7 (IRF7) inhibition reverts age induced transcriptional and metabolic derangement

S.S.D. BIO/13

Coordinator: Prof. Franco Tagliaro

Tutor: Prof. Mirco Galié

Doctoral Student: Dott.ssa Alice Nodari

"Interferon Regulatory Factor 7 (IRF7) inhibition reverts age induced transcriptional and metabolic derangement" – Nodari Alice

Tesi di Dottorato

Sommario

L'invecchiamento si basa sull'accumolo di alterazioni in cellule e tessuti che contribuiscono a deteriorare le funzioni degli organi e portano progressivamente alla morte. Mostriamo qui che la mezza età determina una massiccia riprogrammazione trascrizionale e metabolica, che ricapitola l'attivazione ectopica di una risposta anti-virale intracellulare e altera le funzioni biologiche alla base dell'omeostasi cellulare e della longevità, ovvero la biogenesi mitocondriale e degli aminoacidi. Analisi trascrizionali hanno indicato IRF7 (Interferon Regulatory Factor 7) come principale responsabile di questi cambiamenti, rivelando un ruolo di IRF7 nelle principali alterazioni trascrizionali, mitocondriali e aminoacidiche associate all'età. Abbiamo scoperto che l'inibizione dell'IRF7 è sufficiente per ripristinare il profilo trascrizionale dell'invecchiamento cellulare, determinando riduzione dell'attivazione dell'interferone, riassestamento del profilo trascrizionale, ripristino della funzione mitocondriale e ristabilimento parziale degli aminoacidi. I nostri risultati rivelano che l'IRF7 è il principale regolatore delle alterazioni trascrizionali e metaboliche legate all'invecchiamento e lo indicano come un candidato ideale per lo sviluppo di terapie efficaci contro l'invecchiamento e le malattie legate all'invecchiamento.

Abstract

Aging relies on incremental alterations of cell and tissue which contribute to deteriorate organ functions and progressively drives to death. We show herein that midlife brings about a massive transcriptional/metabolic reprogramming, reminiscent of a cell-autonomous activation of an ectopic anti-viral response, which impairs the biological functions on the basis of cell homeostasis and longevity, namely mitochondrial and amino acid biogenesis. Integrated transcriptional analyses indicate IRF7 to be the major driver of these changes reveling an unprecedented, cell-autonomous role of Interferon Regulatory Factor 7 (IRF7) in leading transcriptional, mitochondrial and amino acid alterations with age. We found that the inhibition of IRF7 is sufficient to revert the transcriptional profiling of "old cell", determining diminished interferon signaling, reverted transcriptional derangement, restored mitochondrial function and partially reestablish the amino acid pool. Our results reveal IRF7 as a major regulator of aging-related transcriptional and metabolic alterations and point it out as an ideal candidate for the development of effective therapies against aging and aging-related diseases.

Table of contents

Introduction

Aging is the progressive functional decline of cells and tissues that affects living organism. Its detrimental effects manifest as early as in the "midlife" (around 12 months of age in rodents) in the form of molecular changes and degenerative phenotypes, which erode the body fitness and increase the risk of multiple pathogenic outcomes. These includes dysregulated inflammatory response [1,2], impaired cardiac and skeletal muscle function [3], altered social and cognitive behaviour [4], increased sensitivity to oxidative stress [5], lipodystrophy [6], cellular senescence [7,8] insulin resistance [6], loss of noradrenergic neurons [9], depression, cancer [10] and so on. The variety of the way aging might manifest throughout the adult life suggests that the impact of the passing time does consists of the wide-spread loose of regulatory mechanisms which coordinate major biological functions [11].

Varied theories have been proposed over the years to conceptualize the systematic occurrence of the aging phenotypes throughout the adult life. All these theories rely on solid experimental evidences and are not mutually exclusive. Reasonably, these theories just reflect some aspects of aging but still fail to explain the complexity of aging and to unveil the biological players that stand on the top of the causal hierarchy of events which drive aging and aging-related diseases.

Owing to the increasing impact of aging on the industrialized world (more than 20% of EU population are estimated to be over 65 by 2025 [12]), the elucidation of the events upstream of the mechanistic queue of aging-related phenotypes is amongst the major scientific challenges of the third millennium.

At the origin of aging: the aging theories

Hallmarks of aging

Nine tentative hallmarks have been enumerated that represent common denominators of aging in different organisms, with special emphasis on mammalian aging. These are: genomic instability, telomere attrition, epigenetic alterations, loss of proteostasis, deregulated nutrient-sensing, mitochondrial dysfunction, cellular senescence, stem cell exhaustion, and altered intercellular communication[13]. These hallmarks co-occur during aging and the understanding of their exact causal network is yet a challenge. The proposed interconnections pose at the basis of aging genomic and mitochondrial DNA, telomere loss, epigenetic drift, and defective proteostasis. These alterations, on

turn, reprogram the hallmarks originally designed for protecting the organism from damage or from nutrient scarcity, such as nutrient sensing, mitochondrial integrated signalling and cellular senescence. The exacerbation of such responses subverts their purpose and generate further damage. This is the case for senescence, which protects the organism from cancer, but in excess can promote aging; similarly, reactive oxygen species (ROS) mediate cell signalling and survival, but at chronic high levels can produce cellular damage; likewise, optimal nutrient-sensing and anabolic pathways are obviously important for survival but in excess and on a long term may become pathological. Finally, defects in compensation mechanisms, due to the accumulation of the alterations described above, results in stem cell exhaustion and altered intercellular communication. This deleterious network leads ultimately to the functional decline of tissue homeostasis associated with aging [13].

However, while all these common denominators of aging are well characterized, it is not definitely accreted which molecular event, if any, might trigger the chain reaction of deleterious pathways that lead to these aberrant phenotypes and their hierarchical causal interconnection.

Oxidative damage

The free radical theory postulate that the production of intracellular reactive oxygen species (ROS) is the main determinant of life span[14]. This theory is based on the structural damage-based hypothesis that age-associated functional losses are due to the accumulation of oxidative damage to macromolecules (lipids, DNA, and proteins)[15]. Mitochondria are thought to be the major source of free radicals, because intra-cellular ROS are by-products of oxidative phosphorylation process. Also, mitochondrial ROS are important in various redox-dependent signalling process[16]. Recently, the mitochondrial free radical theory of aging has been reconsidered due to the observation that increased ROS may prolong lifespan in yeast and C. elegans [17]. In mice, genetic manipulations that increase mitochondrial ROS and oxidative damage do not accelerate aging [18]. Many recent tests of the oxidative damage theory have proposed that somatic cells accumulate molecular damage because they do not need to repair damage completely, inasmuch repair mechanism should be good enough to ensure that death occurs for different reasons[19]. Such tests have triggered a new phase in which fundamental assumptions about aging are being re-examined and new concepts are emerging.

Hyperfunction theory

Among these new concepts, the hyperfunction theory opposes the damage/maintenance paradigm. According this theory, processes that contribute to early-life fitness through growth and reproduction continue in later life at too high level leading to pathology and eventually to death [20]. In humans canonical aging changes are related to developmental programs that are constantly turned-on over adulthood, thus becoming hyper-functional and damaging. These include accumulation of fat, increased blood pressure, glucose and lipoproteins, increased function of platelets, cellular hyperplasia and hypertrophy (which manifest as tumours, atherosclerosis, hypertension, thrombosis) [21]. This suggest that once a program for development is completed, it is not switched-off, even if its continuation is harmful. The switch that would turn-off the developmental program is not selected, because most animals die from accidental death before they have a chance to die for aging or simply because there is no selective pressure against it. This undirected continuation of program is referred as "quasi-program" [22].

Consistent with this point of view, the developmental processes are not the only ones that are not switched-off. Other biological functions, which are essential in timely contexts, may turn detrimental with age. Altered bioenergetics, proteostasis and inflammatory states are the most relevant paradigm. Mis-regulated coordination of these states drives the midlife "switch" toward aging and aging-related [13,23,24].

Deregulated gene expression

The cell fate commitment during eukaryotic development relies on the coordinated and stable expression of restricted cohorts of genes in specific cell populations. There is mounting evidence that aging is marked by the progressive loose of transcriptional coordination, that impairs the core activation program of cells [25]. This trend was shown by studying gene expression both in single cells [25–29] and at the coarse tissue resolution [30], in the stoichiometry between pathway components [31] and in differential analysis of gene co-expression networks [32] . At the single-cell level, the transcription of individual genes is associated with noise, random molecular cell-to-cell fluctuations that create variability in the levels of gene expression within a cell population [33,34]. This phenomenon is intrinsic in development, which is a sequence of transitions between cell states. Both intrinsic factor (the transcriptional history of a cell) and extrinsic factor (intercellular signal) can contribute to transcriptional noise, so transcriptional

regulation itself affects noise in gene expression [35]. Single-cell data indicate that noise in gene expression increases with age leading to the loss of cell-identity at single cell level [26,29]. As consequence, protein production is also subject to stochastic fluctuations. The increased noise in gene expression with age, at both transcriptional and translational levels, leads to decreased organismal fitness, thus is subject to natural selection [36]. As the noise is an intrinsic feature of biological systems, cells play out mechanism to control it[33]. To reduce noise in translation, which would cause serious fluctuation in signalling cascade, cells enhance transcription rate. However, this kind of regulation is very expensive since high energy phosphate groups were hydrolysed to drive the synthesis of little-used transcripts. Therefore, the trade-off is between energy efficiency and noise minimization[37]. Thus it is expected to be advantageous only when the benefit of reducing noise outweighs the cost, like when the coordinated production of the subunits of multi-proteins complexes is needed[36,37]. Cell-to-cell transcriptional noise matches with increased variability in repressive chromatin marks with age. Sporadic loss of silencing of transcriptionally inactive genes may be one of the molecular mechanisms that results in changes in gene expression programs with age [27]. Epigenetic mechanisms are subject to profound rearrangements during aging [13]. Epigenetic changes involve alterations in DNA methylation patterns, post-translational modification of histones, and thus chromatin remodelling. The changes in the epigenetic state and in the transcription that occur during aging are strongly interconnected, for example the up-regulation of the interferon response pathways with age is accompanied by increased transcription and chromatin remodelling at specific endogenous retroviral sequences [38,39]. Perturbation in chromatin modifying enzyme can extend lifespan in invertebrate model[38], suggesting that loss of chromatin homeostasis drives aging. Moreover, histone post transcriptional modifications, such as acetylation or methylation, are involved in cell integrated nutrient sensing and metabolism. For instance, increasing lipid oxidation generally increases histones acetylation[40] and histone acetylation patterns are susceptible to alteration of key metabolites such as acetyl-CoA and NAD^+ [41].

On the other hand, one effect of aging is to diminish the coherence in expression of gene pathways across different tissues. This means that as an organism ages, some genes in a pathway may not be fully activated in tissues that require the function of the pathway, and other pathway components may not be fully repressed in tissues in which

the function of the pathway is not needed. The clusters that loose correlation with age include genes related to mitochondrial function, transcriptional regulation, and ribosome biogenesis [32]. Rangaraju et al. [31] has described the mis-regulation of transcription during aging as "transcriptional drift", an evolutionarily conserved phenomenon in which the expression of genes changes in opposing direction within functional groups. This leads to a progressive loss of mRNA stoichiometry and expression patterns resulting in functional decline with age.

Mitochondrial dysfunction

The impairment of mitochondrial function is one of the major hallmark of aging [13,42] and it has even been postulated to be the general cause of diseases[43]. As cells and organisms age, the efficacy of the respiratory chain tends to diminish, thus increasing electron leakage and reducing ATP generation[44]. The decline of mitochondrial integrity as a function of age was thought to result from the proximity of mitochondrial DNA (mtDNA) to the source of oxidant and the lack of any protective histone covering. mtDNA damaging in turn should cause further mitochondrial deterioration and global cellular damage[45]. However, the decline of mitochondrial function starts early in adulthood, before the cumulative effects of oxidants can become deleterius[46].

Besides to be the house of oxidative phosphorylation, mitochondria are organelles involved in a wide range of cellular processes as programmed cell death, calcium homeostasis and biosynthesis of amino acid, lipids and nucleotides. Not surprisingly, the cell has evolved numerous integrated pathways, known as Integrated Stress Response (ISR), to preserve the quality and function of this organelle in order to guarantee cell homeostasis over fluctuating environmental stress factors [47–50]. ISR is activated in response to diverse stimuli to restore cellular homeostasis, such as hypoxia, amino acid deprivation, glucose deprivation, and viral infection [51,52], which lead to a global decrease in protein synthesis and the induction of selected genes that together promote cellular recovery. Most of these selected genes encode for mitochondrial components [48–57]. Mitochondria are not only targets effectors of the ISR. As all these mechanisms manly rely on nuclear-encoded proteins, mitochondria have evolved the capability to instruct nuclear transcription in response to stress conditions (mitochondrial retrograde response)[58,59]. Also, mitochondria have a multiple mechanism that allow them to activate signalling pathways in the cytosol including

AMP/ATP ratio, release of ROS and TCA cycle metabolites, as well as the localization of immune regulatory proteins on the outer mitochondrial membrane [16,60].

Inflammaging

A common feature of aging tissues is chronic inflammation. "*Inflammaging*" describes the low-grade, chronic, systemic inflammation in aging, in the absence of overt infection ("sterile" inflammation)[1]. Inflammation can be beneficial as an acute, transient immune response to harmful conditions such as traumatic tissue injury or an invading pathogen. This response also facilitates the repair, turnover, and adaptation of many tissues. However, chronic inflammation, usually of low grade and persistent, which occurs without any infection or trauma, results in responses that lead to tissue degeneration [61]. When properly activated to counteract infection, inflammation provides beneficial condition which overweighs possible non-adaptive detrimental effect. But in aging, the balance in this trade-off is shifted, making a non-adaptive trait an unavoidable detrimental consequence [1]. Epidemiological evidence reveals that a state of mild inflammation, marked by elevated levels of inflammatory biomarkers such as C-reactive protein and interleukin-6 (IL-6), is associated and predictive of many aging phenotypes—for example, changes in body composition, energy production and utilization, metabolic homeostasis, immune senescence, and neuronal health [62]. It is increasingly appreciated that chronic inflammation is an important component of numerous disease states including obesity, type 2 diabetes, atherosclerosis, asthma, and neurodegenerative diseases [63] all of which are characteristic disease of aging [15]. Principal sources of inflammaging have been identified and can be grouped as follow: damaged macromolecules and cells (self-debris), which accumulate with age due to increased production and/or inadequate elimination and stimulates innate immunity; cellular senescence, which releases pro-inflammatory cytokines (senescence-associated secretory phenotype, SASP); increasing activation of the coagulation system; age-related changes to the immune system (immune-senescence) and defective or inappropriate regulation of the complement pathway, that can lead to local inflammatory reactions [1,64]. All these mechanisms envision a bi-directional cross-talk between aged tissues and systemic immunity, which sustains a persistent, low-grade inflammatory state.

Cell-autonomous immunity

Besides systemic immunity, which requires the coordinated action of highly specialized immune cell populations, nature has evolved cell-intrinsic, anciently conserved mechanisms of self-defence, which endow non-immune cells with an autonomous capability to counteract infections. This ancient and ubiquitous form of host protection is termed cell-autonomous immunity and operate across all three domains of life [65]. The initial sensing of infection is mediated by pattern-recognition receptors (PRRs) of innate immune system. These receptors recognise pathogen-associated molecular patterns (PAMPs) and danger-associated molecular patterns (DAMPs) as microbial structural components, nucleic acid and proteins. PRR ligation triggers intracellular signalling cascades that induce the expression of pro-inflammatory cytokines and chemokines, type I Interferons (IFNs) and co-stimulatory molecules [66]. A crucial role in these cascades is played by mammalian interferon regulatory factors (IRFs). IRFs are a family of nine transcription actors (IRF1, IRF2, IRF3, IRF4, IRF5, IRF6, IRF7, IRF8, IRF9) that transmit signal to chromatin through the transcriptional activation of type I interferon, which on turn instructs the expression of thousands of interferon-stimulated genes (ISG) for immune cell activation [67].

It has been recently shown that aging associates with an abnormal activation of IFN signalling pathways [38,39,68] although the mechanistic consequences of this activation and their impact on aging phenotype is not clear.

Mitochondria and amino acid biogenies as "core longevity" pathways

The study of the mechanism underling the beneficial effects of "life-extending" interventions, such as dietary restriction, might provide useful information about the pathways the alteration of which is at the "core" of aging phenotypes. Common outcome of these interventions is the enhanced transcription of specific mRNAs despite a general global reduction of protein synthesis. Over-translated mRNAs are those encoding for mitochondrial components and for transcription factors such as ATF4, which promote the transcription of genes mainly involved in amino acid biosynthesis. As such, mitochondrial and amino acid biogenesis can be viewed as "core longevity" pathways that must be finely tuned at transcriptional, translational and post-translational level and may reconfigure in response to the diverse inputs to finally maintain cell homeostasis.

The viral paradox of stress response pathways

Viral infection is enlisted among the factors that trigger the ISR. However, the role of ISR in the case of viral infection is paradoxical. Viruses are fully reliant on the bioenergetic and biosynthetic machinery of the host for the replication of their own components, thus they have evolved complex systems to take control of cellular synthesis machinery. Viruses can cause a shift to aerobic glycolysis to generate rapidly ATPs and accelerate synthesis of both amino acid and fatty acids that are needed to assembly viral progenies. Hence the stress response mechanisms responsible for maintaining homeostasis are exploited to enhance mitochondrial biogenesis and proteins synthesis and paradoxically subverted to meet the viral needs [69]

Cells have evolved IFN signalling as part of their cell-autonomous self-defence pathways to face viral propagation. IFN instructs the transcriptional reprogramming of thousands of genes (Interferon Stimulated Genes, ISG), the impact of which on both the viral and host biology is only partially understood [56,69]. To directly target viral components, interferons and ISGs exert profound effects on cellular metabolism. When the infection is eradicated the INF signalling ceases and the cellular homeostasis should be restored. However, if the INF signalling activation becomes chronic, the deleterious effects would outweigh the benefits by establishing a state of inflammation and deteriorating the cell. Recent studies have started to illuminate on the specific role of interferon in rewiring cellular metabolism and counteract viral infection[70].

Thesis purpose

Despite many decades of studies have contributed to elucidate multiple aspects of aging, a comprehensive picture which might reconnect all these aspect within a unique biological paradigm is still lacking.

Herein, we provide evidence that the cell autonomous up-regulation of Interferon Regulatory Factor 7, the master activator of IFN signalling, impairs mitochondrial and amino acid biogenesis with age and its inhibition at midlife is sufficient to revert the major aspects of aging phenotype, such as altered INF activation, transcriptional derangement, mitochondrial dysfunction and impairment of amino acid biogenesis.

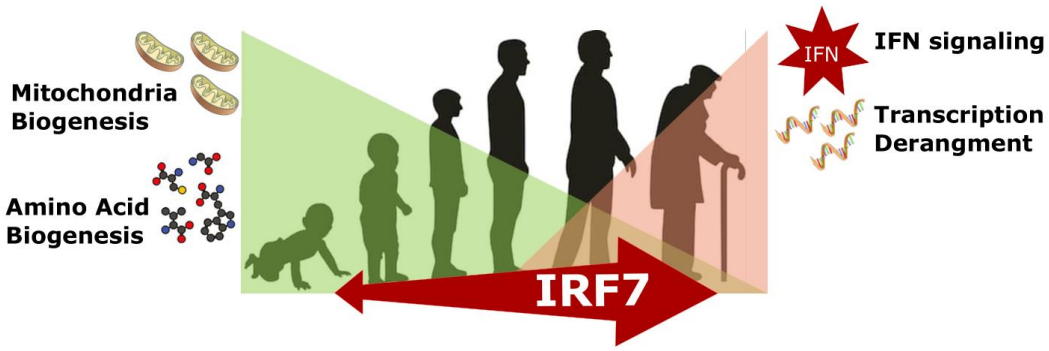

Results

Aging causes a wide-spread transcriptional derangement

Previous studies indicate that the main changes that lead to aging in humans occur during adulthood, when longevity-related pathways are subjected to "midlife" switch[24]. Likewise, most age-related metabolic and neurodegenerative dysfunctions occur within the first half of life (12 months of age) in rodents[3–7,24,50]. Mesenchymal stromal cells (MSC) represents a reliable model to study the impact of aging on cellular function[71]. Hence, in a search for molecular pathways potentially relevant in cell degeneration with age we performed a whole-genome transcriptional profiling of adipose-derived MSC explanted from the inguinal fat pad of 1 (1mo) and 12 months (12mo)-aged mice. To identify functional categories of genes which changed with age in a coordinated manner, we applied a Gene Set Enrichment Analysis (GSEA)[72], which is a computational method that determines whether one or more *a priori* defined set of genes (gene sets) shows statistically significant, concordant differences in expression between two biological phenotypes (Figure 1).

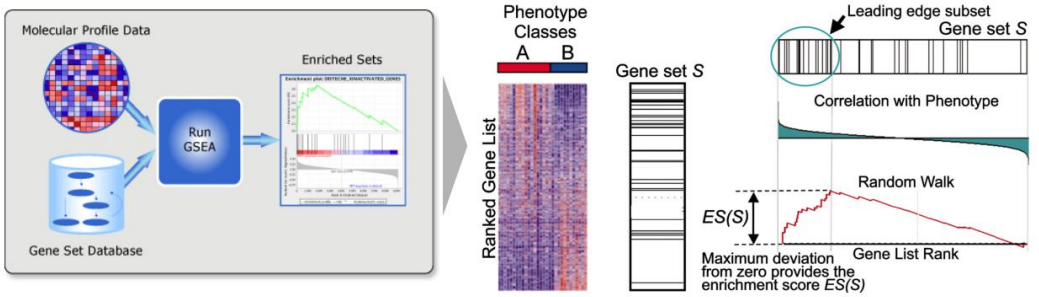

Figure 1: GSEA algorithm sorts genes of the dataset by correlation with phenotypes and then it walks down the list increasing a running-sum statistic when it encounters a gene of the gene set of interest and decreasing it when it does not. The enrichment score (ES) is the maximum deviation from zero encountered in the random walk; it corresponds to a weighted Kolmogorov–Smirnov-like statistic. ES>0 indicates that gene set is enriched in phenotype class A, ES<0 indicates that it is enriched in phenotype class B. Normalized enrichment score (NES) for each gene set is calculated as the ratio between ES and the mean value of ES against all permutations of the default. It accounts for differences in gene set size and in correlations between gene sets and the expression dataset; therefore, NES can be used to compare analysis results across multiple gene sets Besides the ES, GSEA algorithm provides additional output parameters which identify the percentage of genes contributing to the enrichment result (leading edge analysis) and measure whether they are either concentrated on the extremities or spread through the ranked list of dataset genes[72].

We run GSEA on our microarray dataset of differentially aged MSC using multiple collections of pre-compiled gene sets belonging to the Gene Ontology pathways (GO) and varied pathway databases (C2- Curated gene sets and H-Hallmarks) provided by the Molecular Signature Database of the GSEA project[73]. Interestingly, the amount of

gene sets enriched in 12mo vs 1mo MSC (ES and NES <0) was markedly higher than that of the gene sets down-regulated (ES and NES >0) (Figure 2).

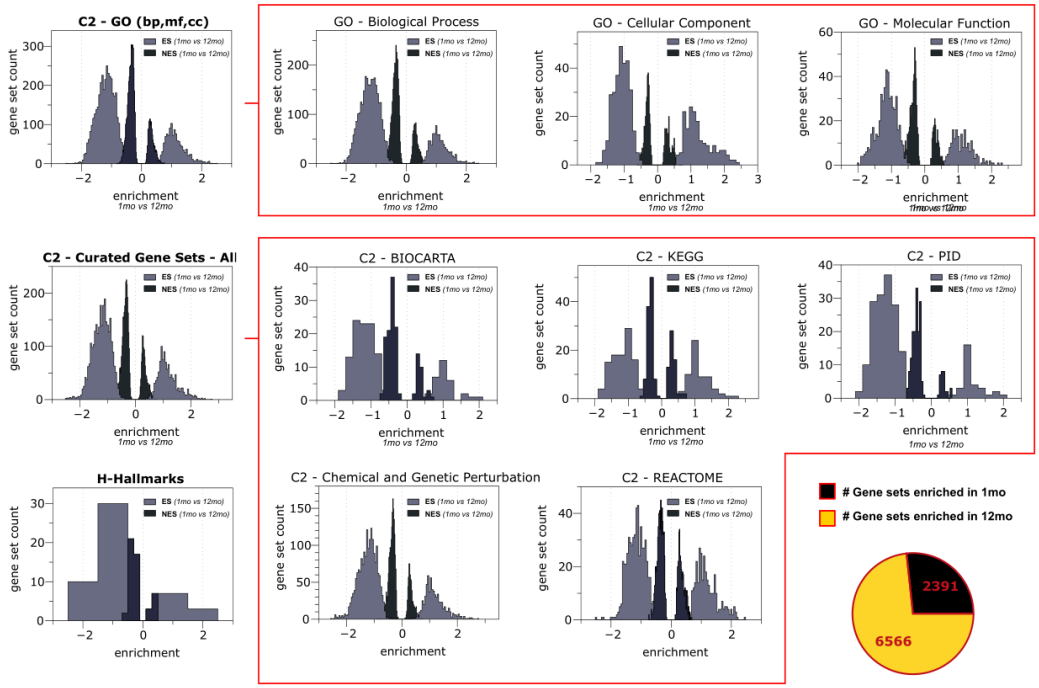

Figure 2: The amount of gene sets from the Molecular Signatures Database (MSigDB), a collection of annotated gene sets for use with GSEA software, enriched (ES<0) in 12 mo vs 1 mo MSC is markedly higher respect the down regulated gene sets. C2: curated gene sets from online pathway databases, publications in PubMed, and knowledge of domain experts (Gene Ontology – biological process, cellular component, molecular function; BIOCARTA, KEGG, PID, chemical and genetic perturbation, REACTOME). H: hallmark gene sets are coherently expressed signatures derived by aggregating many MSigDB gene sets to represent well-defined biological states or processes. Gene sets enriched in 12 mo MSC are 6566 versus 2391 gene sets enriched in 1 mo MSC.

This indicates that genes over-expressed the expression with aging are spread through a wide array of different functional categories, which suggests a functional derangement of gene expression specificity and loose of cell identity. In line with this notion, the distribution plot of the enrichment score values (NES) of the genes sets UP in 12mo displayed a more normal-like shape compared to that 1mo MSC (Figure 3**A**), with much lower value of skewness (which measures the asymmetry of the curve) and kurtosis (which measures how much heavy the tails are and, hence, estimates the weight of outliers relative to the rest of the distribution). This result indicates that while transcriptional pattern in young cells displays higher-than-randomly-expected number of functional categories that are strongly up-regulated, which might reflect functional specialization, this asymmetry fades out with age.

Besides the ES and NES, GSEA provides information about the "leading-edge subset of gene", i.e. the core members of genes that accounts for the ES, and their distributions through the raked list(Figure 3**B**). The percentage of genes contributing

to the ES (Tags) and the spread degree of core genes through the ranked list (Signal) resulted significantly higher in 1mo compared to 12mo MSC, both in absolute terms (Figure 3**C** and **D**) and relative to NES (Figure 3**E** and **F**). Therefore, gene sets enriched in 12mo MSC, although higher in number than those enriched in 1mo MSC, displayed a lower signal strength which indicates that the genes contributing to the enrichment are more spread through the ranked list.

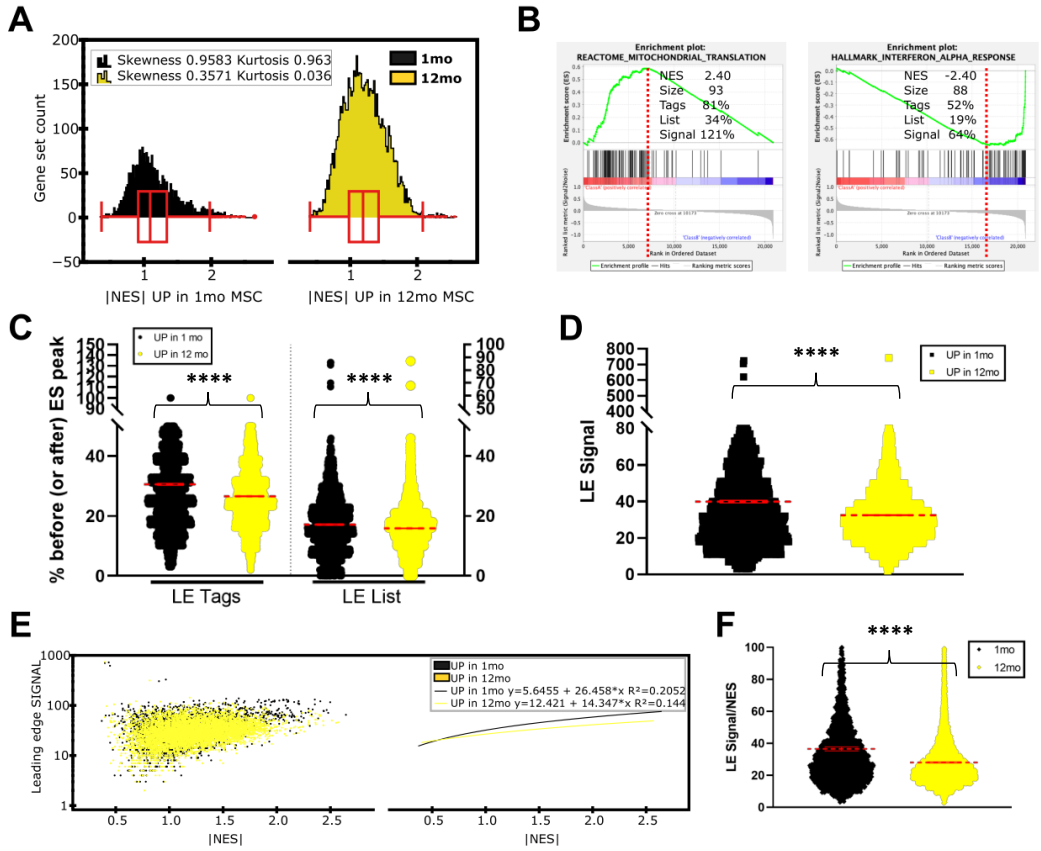

*Figure 3: the distribution plot of the normalized enrichment score values (NES) of the genes sets UP in 12mo compared to that 1mo MSC displayed lower value of skewness (0,3571 in 12mo and 0,9583 in 1 mo) and kurtosis (0,036 in 12mo and 0,963 in 1 mo) (A). Rappresentative enrichment plot of 1mo vs 12mo MSC shows that regardless the NES values, the genes of the gene set might display differen values as regards the leading edge analyis. Tags gives an indication of the percentage of genes contributing to the enrichment score; List gives an indication of where in the list the enrichment score is attained; Signal combines the two previous statistics and the more gene set is spread throughout the list the more the signal strength decreases towards 0% (B). Percentage of Tags (left) and List (right) of all gene sets analysed, mean and SEM are marked in red (C). the enrichment signal strength, that combine Tags and List statistics, of all gene sets analysed, mean and SEM are marked in red (D). Distribution of the signal relative to NES of gene sets UP in 1 mo (black) and UP in 12 mo (yellow) and the respective tendency (E). the enrichment signal strength, that combine Tags and List statistics, normalized for the NES of all gene sets analysed, mean and SEM are marked in red (F). Kolmogorov-Smirnv test: ****p<0,0001.*

Interferon-regulated genes are the most enriched category with age

Amongst the wide array of gene sets enriched in 12mo compared to 1 mo MSC, the top 30 were over-represented by genes set related to the Interferon (IFN) signaling pathway (Figure 4).

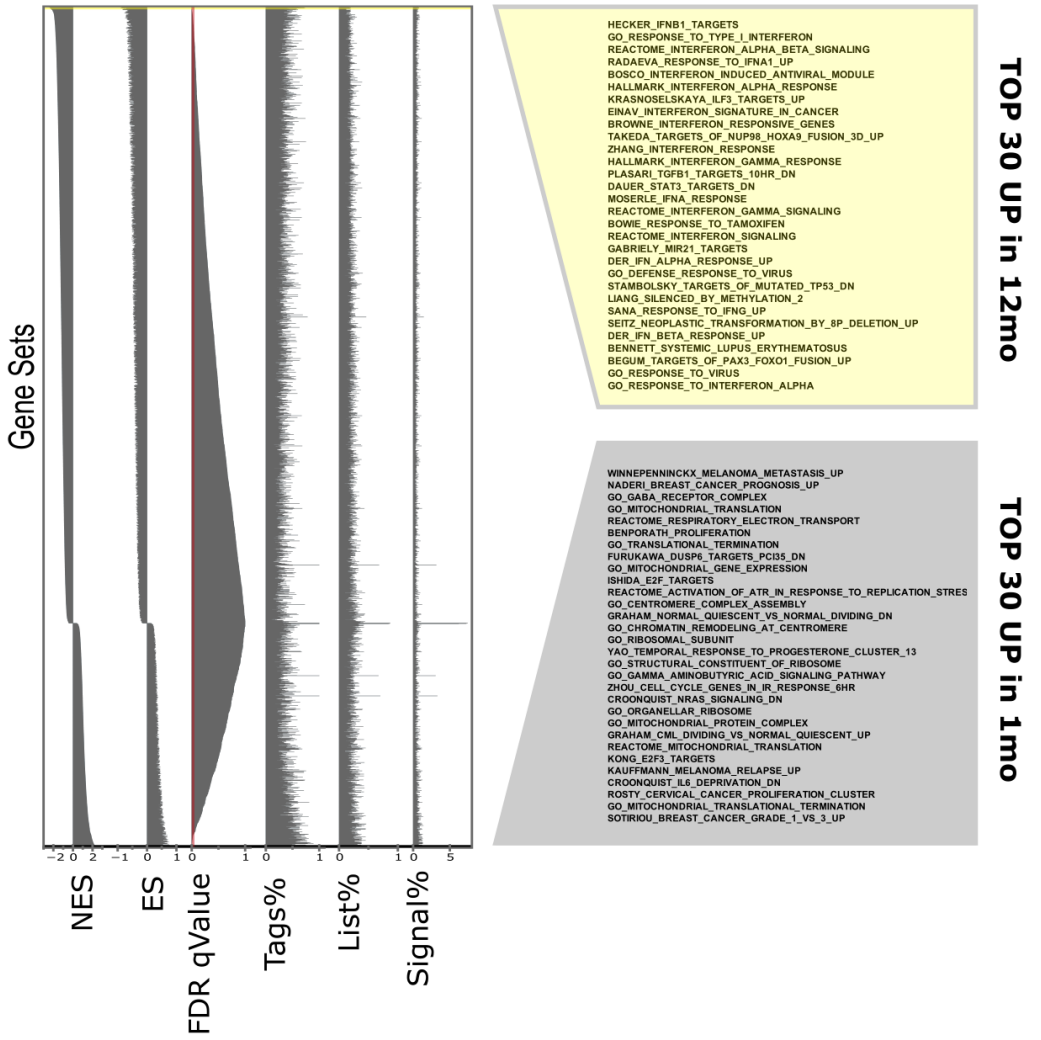

Figure 4: The whole list of gene sets analyzed and ranked by NES value from negative, enriched in 12 mo, to positive, enriched in 1 mo, with the corresponding ES, false discovery rate (FDR) qValue, Tags %, List % and Signal %. Gene sets related to the Interferon (IFN) signaling pathway were the top 30 over-represented in 12mo compared to 1 mo MSC.

In a search for molecular determinants underlying the transcriptional derangement described above, we interrogated our microarray dataset for the enrichment of gene sets comprising the targets of 615 different transcription factors (GSEA c3.tft). The most highly enriched gene sets were related to Interferon Regulatory Factor (IRF) family of transcription factors (Figure 5**A**). Among the nine known members of the IRF family, the only ones readily up-regulated in 12-month-old compared to 1-month-old MSCs was IRF7 and, to a lesser extent, IRF9 (Figure 5**B**). This is in line with the

STRING database [48] which reports IRF7 and IRF9 to display the highest frequency of co-expression (Figure 5**C**). Previously identified IRF7-specific targets [49] were also significantly enriched in older MSCs (Figure 5**D**). Interferon Regulatory Factor (IRF) 7 functions at the interface between innate and adaptive immunity and modulates the expression of type-I interferon (IFN-I) and Interferon stimulated genes (ISGs)[31]. We confirmed a remarkable up-regulation of IRF7 mRNA and protein Figure 5**F**) in 12-month-old compared to 1-month-old MSCs.

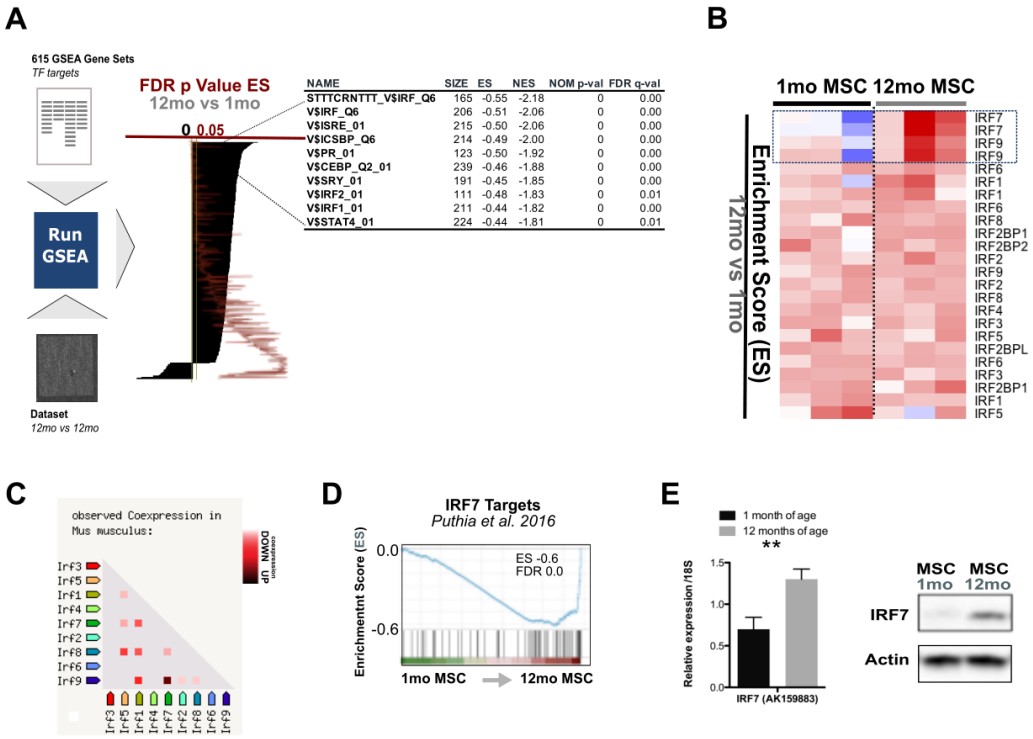

*Figure 5: Using the GSEA algorithm we interrogated the transcriptomic profiles of 1mo and 12mo MSC samples for the enrichment of a precompiled collection of 615 gene sets of transcription factor motifs based on the work of Xie et al(80). Genes upregulated in 12mo vs 1mo MSC were enriched in motifs related to Interferon Regulatory Factors (IRFs) family of transcription factors (**A**). Among the 9 members of the IRF family of transcription factors, IRF7 and, to a much lesser extent, IRF9 were the only ones that were readily up-regulated in 12mo compared to 1mo MSC (**B**). STRING analysis revealed that IRF7 and IRF9 are frequently co-regulated (**C**). 12mo MSC displayed a significantly higher transcriptional expression of genes previously identified as IRF7 targets (**D**) and a higher expression of IRF7 at both transcriptional and protein level (**E**).*

IRF7 increase with age in a tissue specific manner

The increase of IRF7 with age is not restricted to MSC since we found the IRF7 protein to be up-regulated in skeletal muscle (both gastrocnemius and quadriceps), adipose tissue and lungs (but not the spinal cord) of 8-months old mice compared to 1-month old mice (Figure 6**A**). In addition, we surveyed the expression of IRF7 transcripts across multiple publicly available datasets (Figure 6**B**) and confirmed its upregulation at either middle or old age in varied tissues/organs (skeletal muscle,

adipocytes, heart, kidney, brain, pulmonary cells) across multiple species. Exceptions were found for the hippocampus, as different studies provided contradictory results, and hematopoietic stem cells, where IRF7 expression decreases with age.

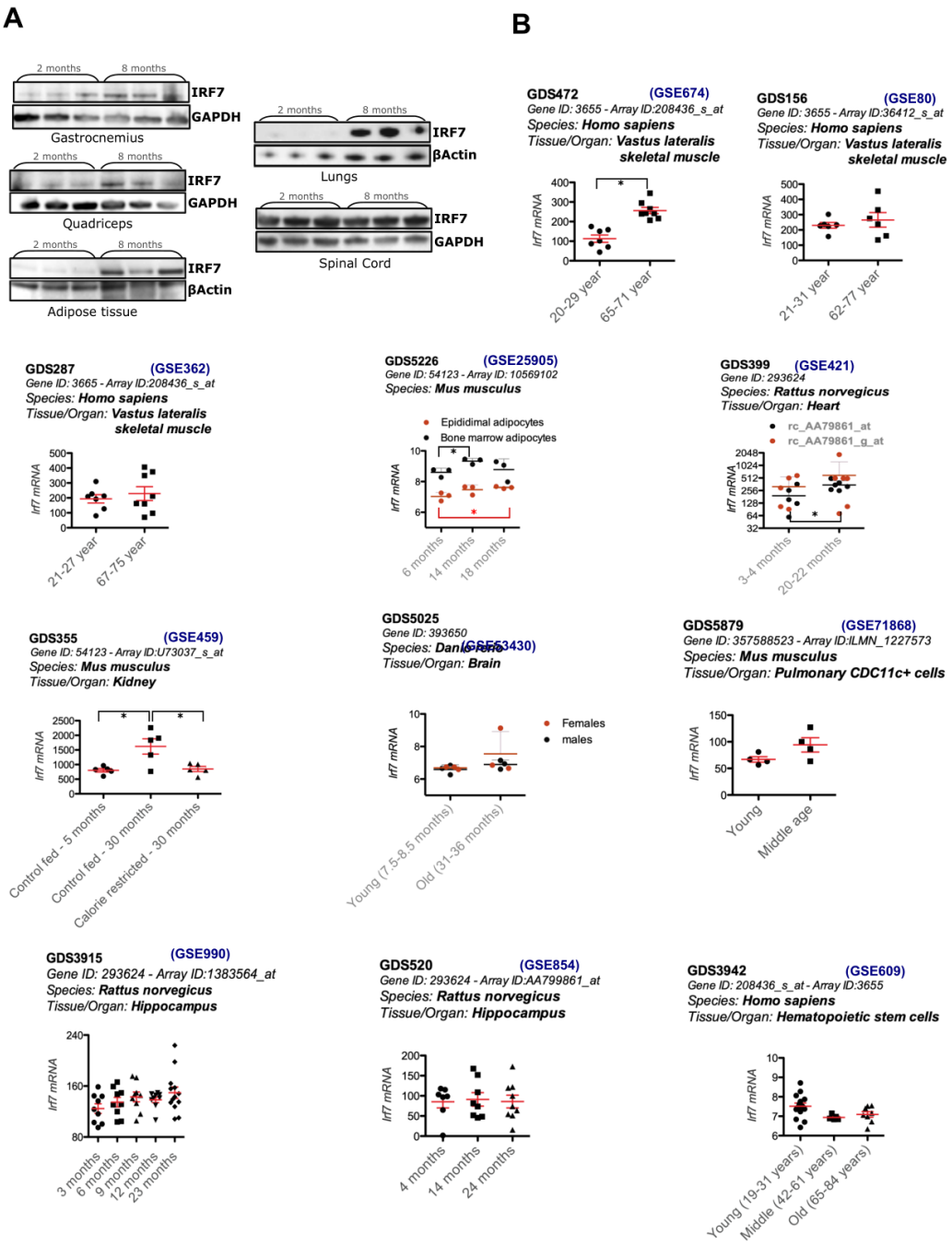

*Figure 6: IRF7 protein resulted increased in multiple organs (gastrocnemius, quadriceps, adipose tissue, lungs), although not in spinal cord, of 8 months-old mice compared to 1months mice (**A**). IRF7 transcripts proven to be upregulated with age in multiple tissue/organs across multiple species (**B**).*

IRF7 knock-down partially reverts the age-related transcriptional derangement

Collectively, results described above point to the increase of IRF7 as a major trigger of the transcriptional derangement with age. To definitely test this hypothesis, we assessed whether the knock-down IRF7 in 12mo MSC (shIRF7) might revert the age-induced transcriptional changes (Figure 7**A**). In line with our hypothesis, the pattern of fold-change in shIRF7 cells vs control (12mo cells transduced with either empty or scrambled vector) significantly correlated with that of 1mo vs 12mo cells (Figure 7**B**). Half the 20182 transcripts in common between the two arrays were either up-regulated in 12mo vs 1mo and reverted down in shIRF7 (Rev-UP, 27.2%) or down-regulated in 12mo vs 1mo and reverted up in shIRF7 (Rev-DOWN, 23.6%). With the exception of a marginal percentage of genes that did not change with age and were up- or down-regulated in shIRF7 (no-change -UP, 0.08% and no-change-DOWN, 0.13%, respectively), the other half of genes displayed the same trend across the two arrays, i.e. were either up-regulated with age and even up-regulated in shIRF7 or vice-versa (no-Rev-UP, 26.2% and no-Rev-DOWN, 22.7%, respectively) (Figure 7**C**). The count of reverted and non-reverted transcript just reflects a randomly expected fractionation (around 25% each). However, the extent of fold-changes (in absolute values) of reverted transcripts in shIRF7 vs ctrl was significantly higher on average than that of non-reverted transcripts (Figure 7**D**). This indicates that the IRF7 knock-down can revert the age-induced repatterning of gene transcripts.

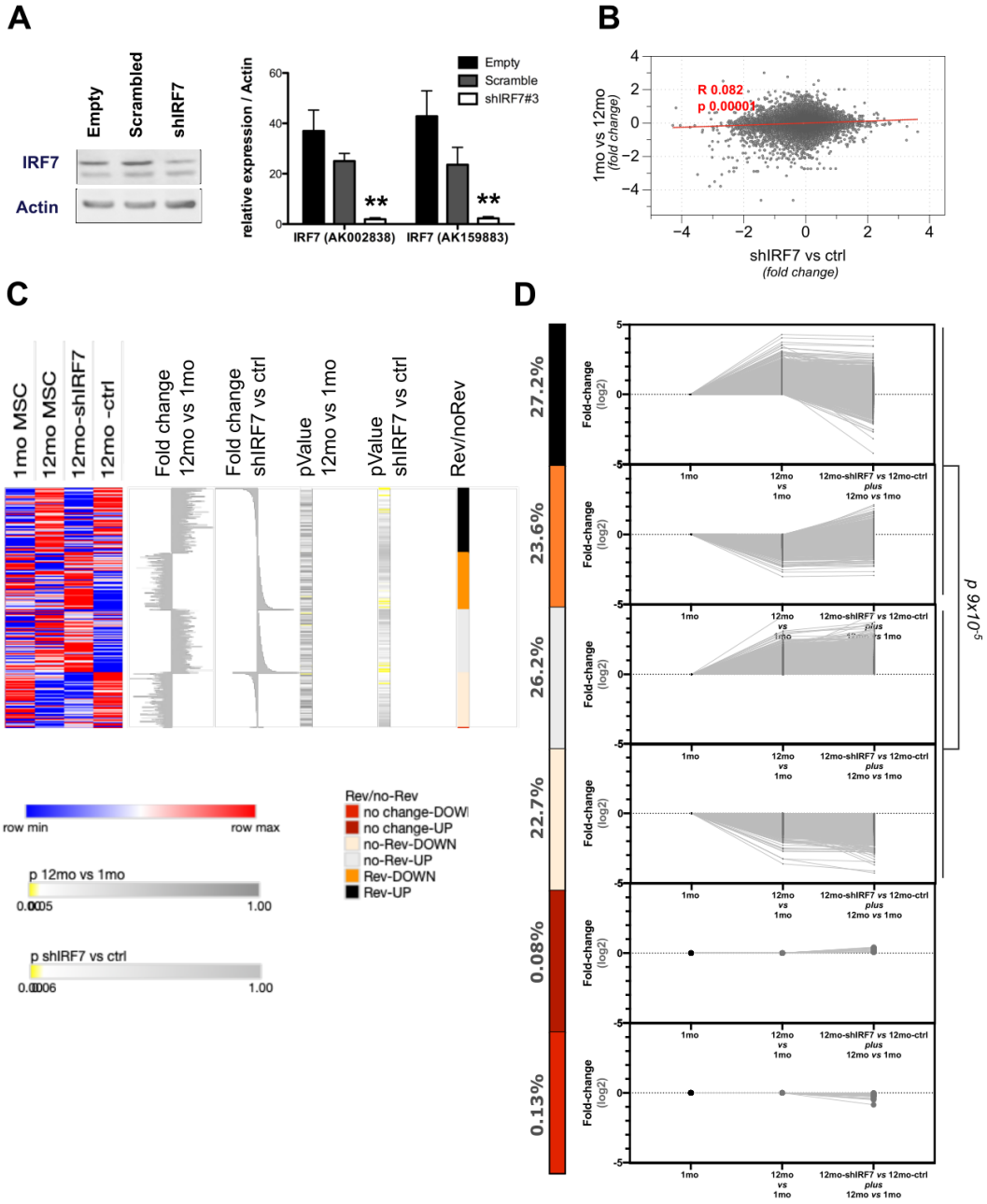

*Figure 7: IRF7 was silenced in 12mo MSC as is shown by western blot analysis (left) and rtPCR (right) 12mo MSC transduced with Empty and shRNA scramble pLKO. vectors were used as controls (**A**). ES values fold change of the REACTOME gene set database between 12mo Ctrl and 12mo shIRF7 were plotted versus the increasingly ranked ES values fold change of the same gene sets between 1mo and 12mo showing a significant linear correlation, red line (**B**). Half of the 20182 transcripts in common between the two arrays have been perturbed after IRF7 silencing. The 27,2 % of these genes were up-regulated in 12mo vs 1 mo and reverted down after silencing of IRF7 (Rev-UP, black). The 23.6% were down-regulated in in 12mo vs 1mo and reverted up in shIRF7 (Rev-DOWN, orange). Among the genes that did not change with age, the 0.08% were up-regulated in shIRF7 (no-change -UP, dark red) and the 0.13% were down-regulated (no-change-DOWN, light red). The other half of transcript displayed the same trend across the two arrays. The 26.2% were either up-regulated with age and even up-regulated in shIRF7 (no-Rev-UP, gray) and the 22.7% were either down-regulated with age and even down-regulated in shIRF7 (no-Rev-DOWN, pink) (**C**). Even though the count of reverted and non-reverted transcript just reflects a randomly expected fractionation (around 25% each), the extent fold-changes (in absolute values) of reverted transcripts in shIRF7 vs ctrl was significantly higher on average than that of non-reverted transcripts (**D**).*

To assess whether it reverts also age-related repatterning of functional gene categories, we run GSEA on shIRF7 vs ctrl dataset, using multiple collection GO, C2- Curated and H-Hallmarks gene sets. The distribution plots of gene set enrichment shIRF7 vs ctrl overlaps those of 1mo vs 12mo, with a larger amount of gene sets enriched in ctrl (NES<0) than in shIRF7 cells (Figure 8).

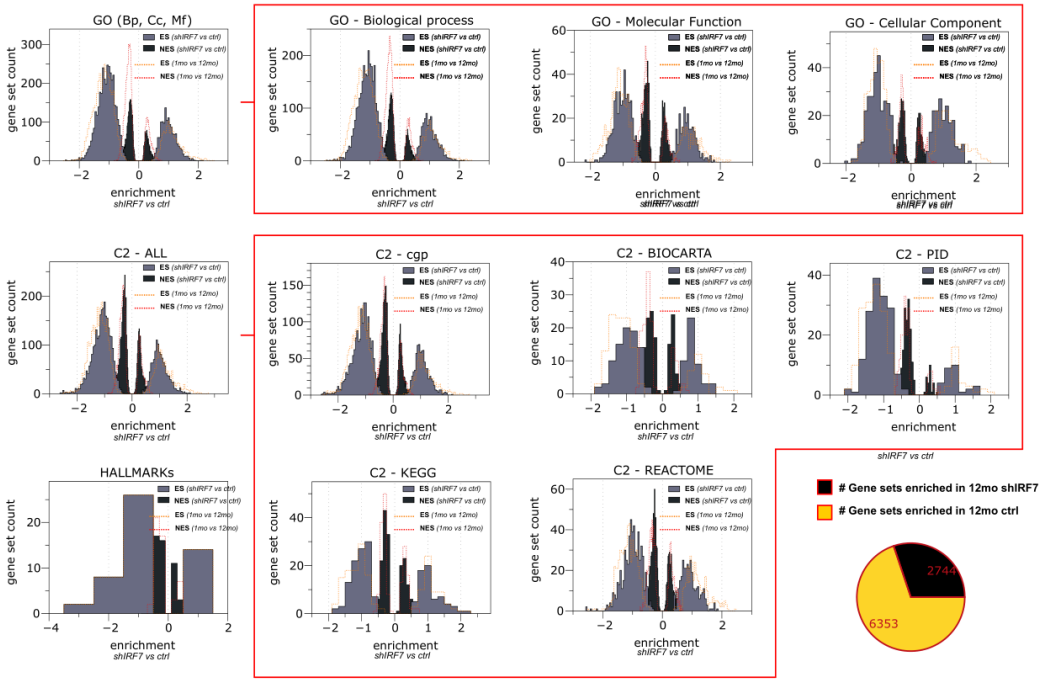

Figure 8: The amount of gene sets from the Molecular Signatures Database (MSigDB), a collection of annotated gene sets for use with GSEA software, enriched (ES<0) in 12 mo shIRF7 vs 12 mo ctrl MSC is markedly higher respect the down regulated gene sets. C2: curated gene sets from online pathway databases, publications in PubMed, and knowledge of domain experts (Gene Ontology – biological process, cellular component, molecular function; BIOCARTA, KEGG, PID, chemical and genetic perturbation, REACTOME). H: hallmark gene sets are coherently expressed signatures derived by aggregating many MSigDB gene sets to represent well-defined biological states or processes. Gene sets enriched in 12 mo ctrl are 6353 versus 2744 gene sets enriched in 12 mo shIRF7 MSC.

Although kurtosis was markedly reduced in the ES distribution plot of shIRF7 vs ctrl (Figure 9**A**), Skewness (Figure 9**A**), Tags (Figure 9**B**), Signal (Figure 9**C**) and Signal/NES (Figure 9**D** and **E**) values were significantly increased. Collectively, these data indicate that the IRF7 knock-down partially reverts the global transcriptional derangement induced by age.

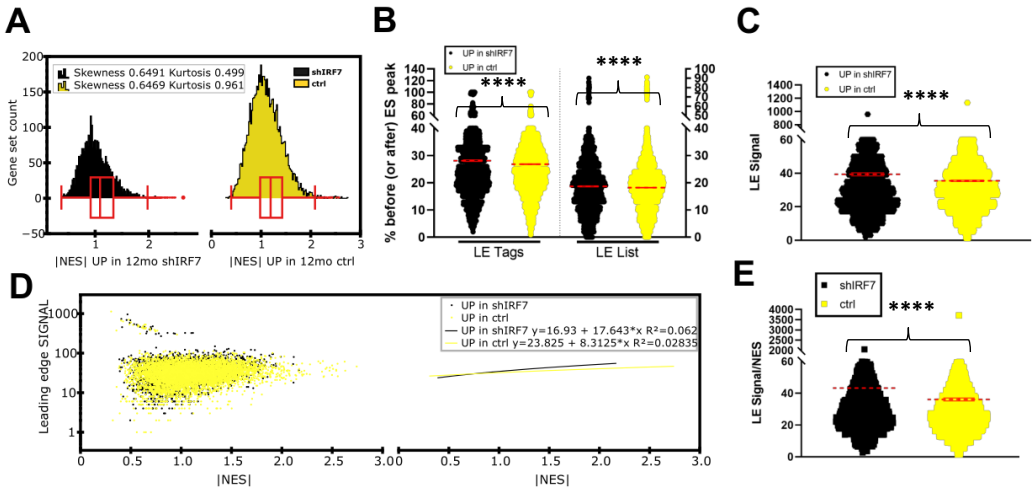

*Figure 9: The distribution plot of the normalized enrichment score values (NES) of the genes sets UP in 12mo shIRF7 compared to that 12 mo ctrl MSC displayed lower value kurtosis (0,499 for shIRF7 and 0,961 for ctrl) but lightly higher values of skewness (0,6491 for shIRF7 and 0,6469 for ctrl) (**A**). Percentage of Tags (left) and List (right) as well gene sets analysed were significantly increased in shIRF7, mean and SEM are marked in red, (**B**) as the enrichment signal strength, that combine Tags and List statistics, of all gene sets analysed, mean and SEM are marked in red (**C**). Distribution of the signal relative to NES of gene sets UP in 12 mo shIRF7 (black) and UP in 12 mo ctrl (yellow) and the respective tendency (**D**). the enrichment signal strength, that combine Tags and List statistics, normalized for the NES of all gene sets analysed, mean and SEM are marked in red (**E**). Kolmogorov-Smirnv test: p<0,001 (****).*

Increased IFN signalling at midlife accompanies the transcriptional reprogramming of genes involved in mitochondrial and amino acid biogenesis

Transcription is the first level of regulation of cell identity and function. Global derangement in gene transcription with age may impact of multiple biological functions. In a search of biological functions which changed the most with age we analysed more in depth transcriptional changes. We found that, while categories related to cytokine and IFN signalling pathways resulted to be the most enriched in 12mo MSC, gene associated to Respiratory Electron Transport and DNA damage response were on the top of the enrichment score (ES) in 1mo MSC (Figure 4 e Figure 10**A**). Additionally, the member of respiratory chain, GSEA of Gene Ontology (GO) [74,75] functional categories demonstrated the significant enrichment in 1mo MSC of a larger repertoire of mitochondrial genes encoding for structural and functional components, including mitochondrial matrix, ribonucleoproteins, aminoacyl-tRNA synthetases and regulators of the mitochondrial biogenesis (Figure 10**B**). Interestingly, amongst the unique transcripts included in the mitochondrial-related gene sets mentioned above, the 71% were identified as IFN targets by the INTERFEROME database, a web-based repository of experimentally verified interferon stimulated genes (ISGs) [76] (Figure 10**C**) and, between these, 221 genes resulted significantly enriched in 1mo vs 12mo MSC.

This suggest that the alteration of mitochondrial genes with age might be secondary to the increase of IFN signalling. Also, these mitochondrial-related genes target of INF signalling are involved in amino acid biosynthesis (Figure 10**C**), which, along with mitochondrial biogenesis, play a fundamental role in the integrated stress response, therefore in the maintenance and regulation of homeostasis and in life-extending interventions such as dietary restriction. We then interrogated multiple publicly

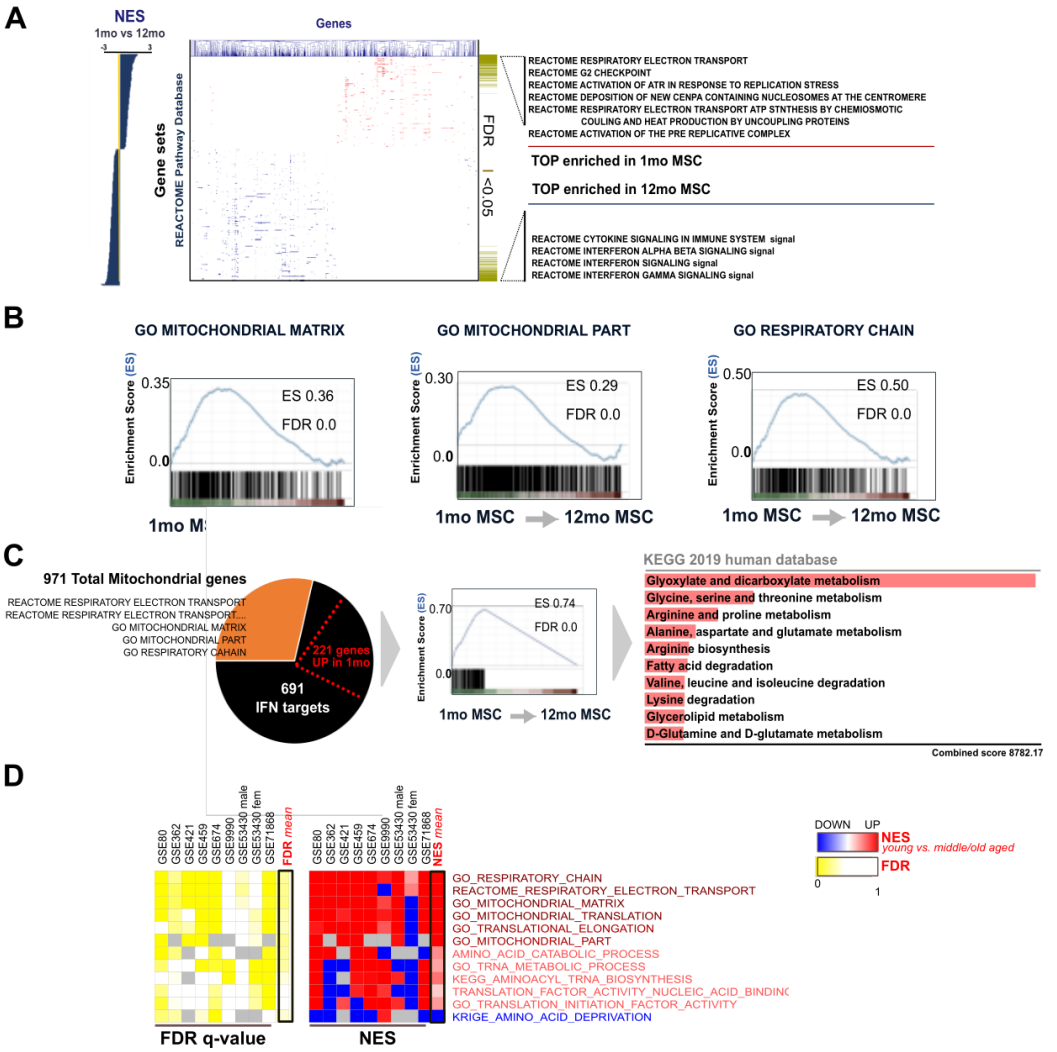

*Figure 10: Microarray dataset of MSC from differently aged mice underwent Gene Set Enrichment Analysis (GSEA) with a pre-compiled collection of 480 gene sets of REACTOME functional category database. Gene sets were ranked according to the Normalized Enrichment Score (NES) values (1mo MSC vs 12mo MSC), which account for differences in gene set size and in correlations between gene sets and the expression dataset. The most enriched gene sets in 1mo MSC were relative to mitochondrial genes and DNA repair mechanisms, while the most enriched in12mo MSC were relative to the interferon signaling pathway (**A**). GSEA using gene sets from Gene Ontology (GO) database, confirmed the massive enrichment of different categories of mitochondrial genes in 1mo MSC compared to 12mo MSC (**B**). The mitochondrial related gene sets comprised 971 unique annotated transcripts. Amongst them, 691 were identified as ISGs according with the INTERFEROME database. 221 out of these 691 were strongly upregulated in 1mo compared with 12mo MSC. These genes were ontologically related with biochemical pathways of amino acid biosynthesis (**C**). GSEA analysis revealed a reduced expression mitochondrial/ translation related gene and an increased expression of amino acid deprivation related genes with age in multiple organ/ tissue of multiple species (**D**).*

available datasets for the enrichment of gene sets related to mitochondrial biogenesis and function, translation and amino acid metabolism (Figure 10**D**). In line with the data achieved on MSC, younger samples across the different datasets displayed a strong enrichment of genes related to mitochondrial components, mitochondrial translation machinery and, to a lesser extent, aminoacyl-tRNA-biosynthesis. Conversely, older samples displayed the enrichment of genes related to the amino acid deprivation.
These results indicate that an increased IFN signalling at midlife accompanies the transcriptional reprogramming of genes involved in mitochondrial and amino acid biogenesis.

Aging impairs mitochondria and amino acid biosynthesis

Quantitative PCR analysis confirmed the over-expression of multiple oxidative phosphorylation (OXPHOS) genes (Figure 11**A**). Consistent with transcriptional analysis, we found a degenerated mitochondria structure in 12mo MSC, while mitochondria of 1mo MSC displayed a significantly larger size and more structured cristae (Figure 11**B**).

Moreover, we compared the untargeted metabolomic profiles of 1mo and 12mo MSC (Figure 11**C**) to assess the observed enrichment of genes responsible of amino acid biosynthesis in younger samples. Consistent with transcriptional data, the widest difference is represented by a drastic depletion in 12mo MSC of a cluster of metabolites functionally assigned to amino acid- related ontological pathways (Cluster1), then strongly enriched in amino acid (Figure 11**C, right panel**). This cluster included glucose and lactate, glycolytic intermediates, and citrate and malate, TCA cycle intermediates, which suggest a reduced glucose metabolic flux in 12mo MSC aimed at providing the intermediates for the amino acid biosynthesis. Also, we found a slight change in fatty acid intermediates (Cluster 2) and a striking increase in 12mo MSC of metabolites that did not match any pre-compiled ontological category (Cluster 3). Among these metabolites we can find cholesterol, which is known to increase with INF activation [77], caprylic acid and nonanoic acid, which are involved in up-regulation of endogenous host defence peptides to enhance the function of intestinal epithelial immunological barrier via histone deacetylase inhibition [78], and amino-malonic acid, which is a known component of atherosclerotic plaques and is suspected to originate from errors in protein synthesis and oxidative damage to amino acid residues in

proteins [79,80]. Collectively, these data correlate with pro-inflammatory phenotype an altered proteostasis with aging.

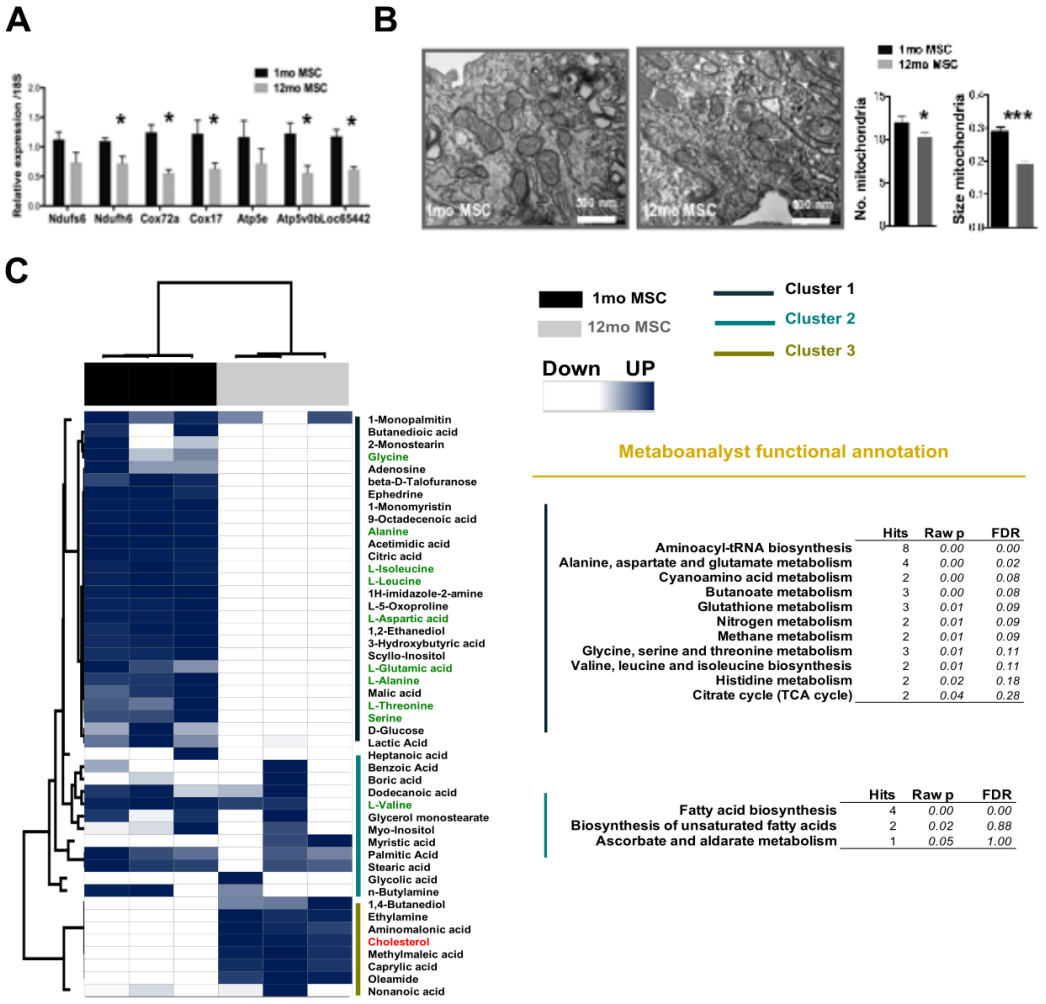

*Figure 11: Aging induces mitochondrial degeneration. qPCR analysis on a higher number of biological replicates (n= 6/group) confirmed the up-regulation of selected mitochondrial genes in 1mo MSC (**A**).Mitochondria were less abundant and displayed a reduced size in 12mo compared to 1mo MSC (unpaired t-test, *p<0.05 **p<0.01 ***p<0.0001) (**B**). Aging suppresses amino acid metabolism. Gas chromatography–time of flight mass spectrometry (GC-TOF/MS) revealed many differences in the metabolomic profile between 1mo and 12mo MSC. On the bases of an unsupervised hierarchical classification (Pearson correlation) we identified 3 clusters of metabolites which proven to be decreased (Cluster 1), unchanged (Cluster 2) or increased (Cluster 3) with aging (**C, left panel**). Functional annotation of these clusters through Metaboanalyst algorithm (79) indicated that metabolites in Cluster 1 were mainly related to amino acid metabolism and translation, while those of cluster 2 were related to fatty acid metabolism. No significant functional enrichment was identified for Cluster 3 (**C, right panel**). Cluster 1 included many amino acids (**C, blue**).*

Aging reduce amino acid biosynthesis

In line with the metabolomic data, we found that many enzymes involved in the synthesis of amino acids were actually up-regulated in the 1mo MSC respect to 12mo MSC, especially those related to the serine and glycine biosynthesis (Figure 12 **A and B**). Interesting, the list includes Asparagine synthetase (Asns), an established result of

the activation of Atf4, which is the common transcriptional effector downstream stress response pathways. We used INTERFEROME database to ascertain if INFs could modulate amino acid biosynthesis and we found that, on the basis of the experimental evidence of the default limit of 2-fold change in expression upon IFN treatment, the

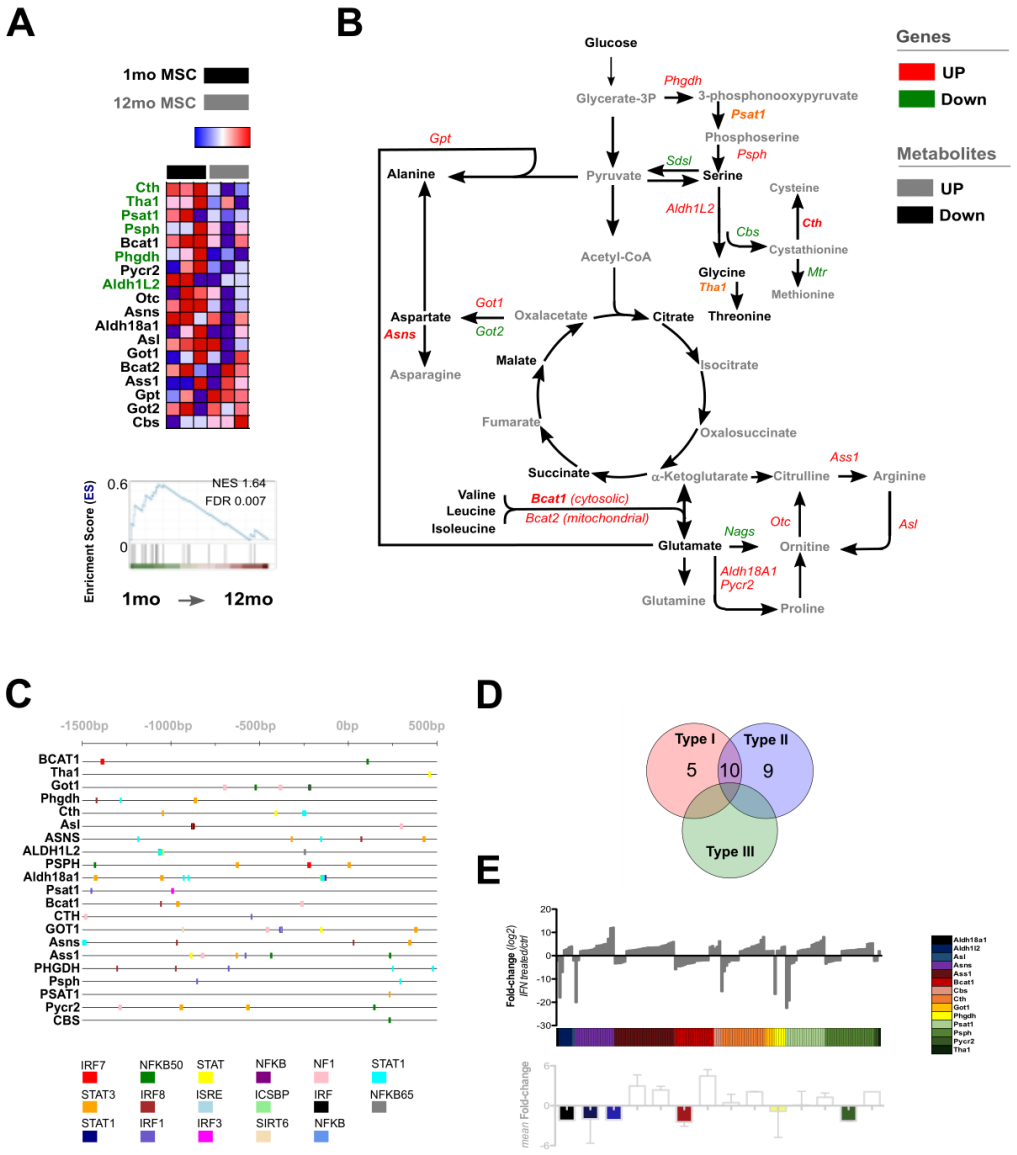

*Figure 12: Gene set enrichment analysis (GSEA) showed a significant enrichment of genes encoding for key enzymes of amino acid biosynthesis in 1mo vs 12mo MSC (**A**), especially those involved in the serine and glycine biosynthesis (**A, green**). Most of these genes were either significantly (**B, red bold**) or not-significantly (**B, red normal**) up-regulated in 1mo, while only 5 out 16 were (not-significantly) down-regulated (**B, green**). AA biosynthesis genes are ISGs. INTERFROME database identified the genes in B (AA biosynthesis genes) as Interferon Stimulated Genes (ISGs), on the basis of experimental data in literatures which reported their expression change (2-fold or higher) upon IFN treatments. INTERFEROME analysis identified IFN-related transcription factors motifs within a sequence spanning from 1500 bp upstream to 500bp downstream the transcription start site of these genes (**C**). These genes resulted to be targets of either Type I or Type II IFN, or both (**D**). 6 out 14 AA biosynthesis genes resulted to be down-regulated on average in the experimental data collected in the INTERFEROME database (**E**).*

amino acid-related genes reported in Figure 12, hereafter referred to as AA biosynthesis genes, are identify as ISGs. These genes displayed motifs of varied transcription factors activated by IFN- type I and II (Figure 12 **C and D**) and only a few of the AA biosynthesis genes are expected to be down-regulated upon IFN stimulation (Figure 12**D**). Amongst them, *Branched chain amino acid transaminase 1* (*Bcat1*) display the strongest down-regulation in 12mo MSC, this gene encodes for the enzyme which catalyses the first, rate-limiting, step of the degradation of the essential amino acids valine, leucine and isoleucine (branched chain amino acid, BCAA). BCAA degradation is a central pathway of amino acid metabolism which may feed the anapleoretic flux of the TCA cycle throughout the alpha-ketoglutarate. Collectively these results suggest that the activation of IFN signalling is causally related to the amino acid depletion we found in our midlife model, although additional aging-related (adaptive) mechanisms might be in place.

Aging enhances amino acid degradation

Besides the transcriptional repression on genes implicated in the amino acid biosynthesis, we found that almost all the major genes implicated in amino acid degradation pathways were slightly but co-ordinately up-regulated in 12mo MSC (Figure 13**A**). The most significant up-regulated gene is the *Indoleamine-pyrrole 2,3-dioxygenase* 1 (*Ido1*), that catalyses the first limiting step of the tryptophan degradation. Tryptophan degradation has long been recognized as a hallmark of aging [81] while its inhibition preserves proteostasis and prolongs life span [82].Consistent with an enhanced IFN signalling with age, Ido1 has been shown to be induced by innate immunity to subtract this essential amino acid from the viral needs [83]. On the contrary, among the amino acid degradation-related genes, the only down-regulated in 12mo MSC were *Indoleamine-pyrrole 2,3-dioxygenase* 2 (*Ido2*), and the two isoforms of the *Branched chain amino acid transaminase* (*Bcat1* and *2*). *Ido2,* unlike its homolog *Ido1,* has been shown to be poorly related to IFN-activation [84], hence its down-regulation herein is not surprising. *Bcat* genes encode for two enzymes, BCAT1 and BCAT2, which catalyse the first step of the degradation of the branched chain amino acids (valine, leucine and isoleucine) (Figure 13**B**). This step generates a-ketoacids (BCKAs) from BCAA and yields glutamate as by-product.

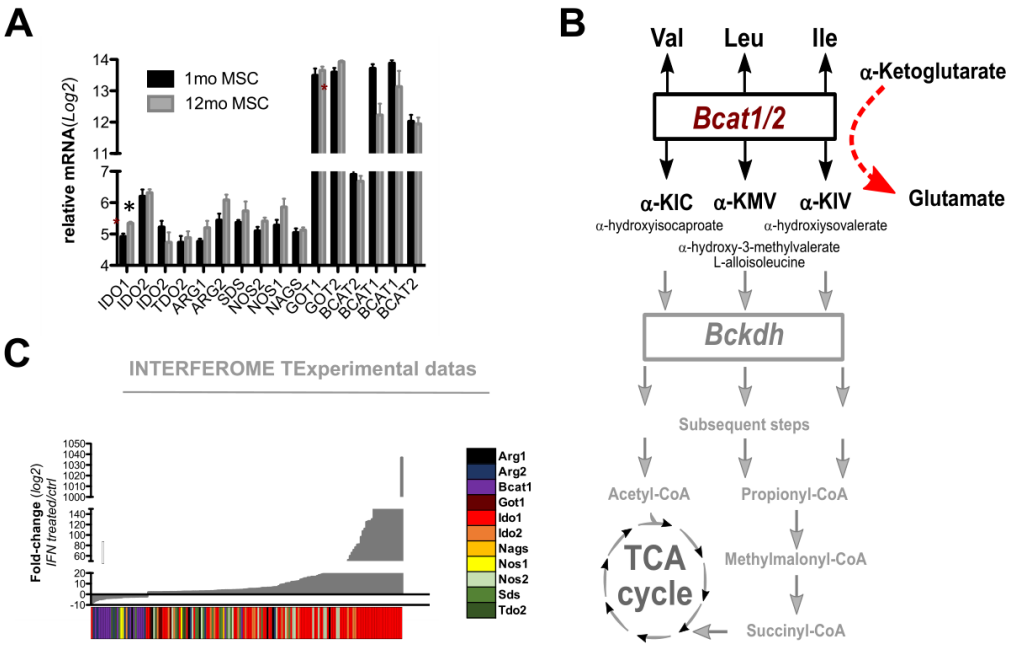

*Figure 13: Genes encoding for the enzymes that catalyzes the amino acid degradation results slightly but coordinately upregulated in 12mo MSC. unpaired t-test, *p<0.05 (**A**), except BCAT1 and 2, which catalyzes the first reversible step of the branched chain amino acid (Val, Leu and Ile) degradation (**B**). These genes are mainly predicted to be up-regulated upon IFN activation according to the INTERFEROME database (**C**)*

The forward and reverse reactions have a low free energy change, thus they are likely in equilibrium in most cases, although glutamate abundance may shift the balance towards the reverse reaction [85], because of the 100-fold higher K_m of BCKAs compared to that of BCAAs. As the amino acid biosynthesis genes, the amino acid degradation genes are identified as ISGs and resulted upregulated upon IFN treatment in multiple experimental setting according to INTERFEROME database (Figure 13**C**). Collectively these data indicate that the activation of IFN pathway enhances amino acid degradation.

IRF7 inhibition reverts the age-related alterations of interferon signal and restore transcriptional expression of mitochondrial genes

At this point we verified if the repatterning of gene transcripts observed as outcome of IRF7 inhibition could also restore aged phenotype described above. To assess which of these gene sets was reversed the most, we subtracted their ES value in 12mo-ctrl vs. shIRF7 to that of 1mo vs. 12mo and ranked them accordingly. Strikingly, interferon signalling pathway and oxidative phosphorylation hit the top up and top down positions, respectively (Figure 14**A**). Genes that were significantly (t-test, $p<0.05$) down-regulated in 12mo-shIRF7 were enriched in functional categories related to

antiviral immune response, thus clearly validating the efficiency of the IRF7 loss of function (Figure 14**B, right panel**). On the other hand, genes significantly up-regulated in 12mo-shIRF7 were predominantly enriched in mitochondrial and electron transport-related genes (Figure 14**B, left panel**).

Also, genes related to "mitochondrial-matrix", "respiratory chain" and "mitochondrial-part" Gene Ontology categories resulted significantly enriched in 12mo-shIRF7 compared to 12mo ctrl cells (Figure 14**C**). These results indicate that IRF7 loss of function massively reverts the transcriptional changes induced by aging. Collectively, the above data point to IRF7 as the causal connection of the increased interferon signalling pathway and diminished mitochondrial/amino acid gene expression with age.

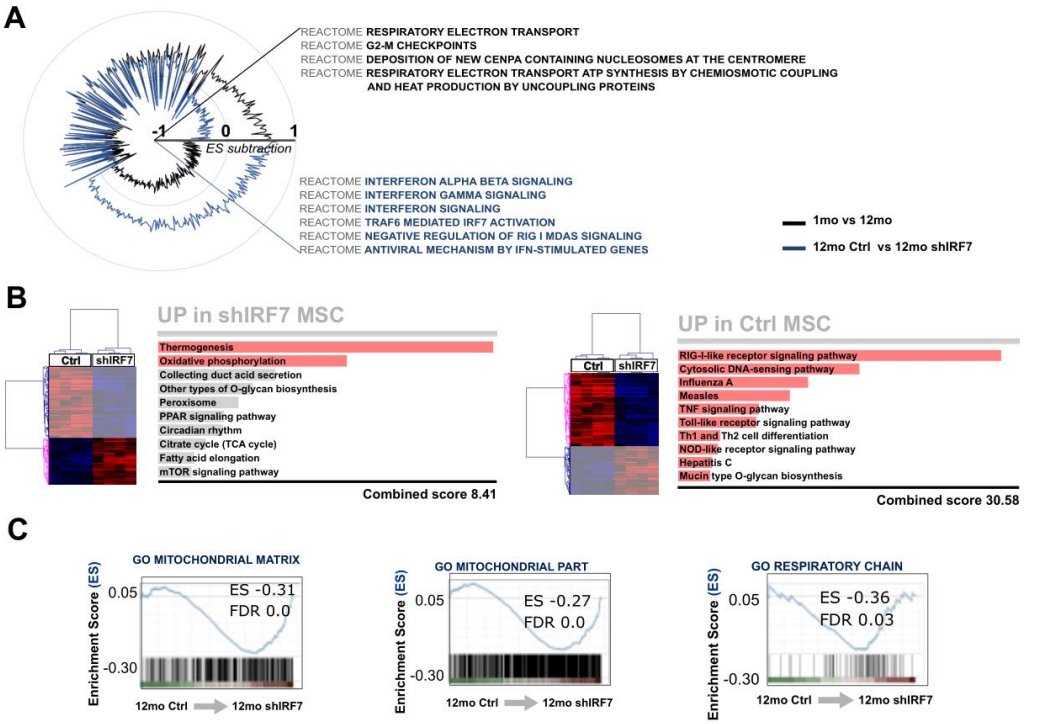

*Figure 14: IRF7 silencing reverts the aging-induced transcriptional changes in MSC. ES values of the REACTOME gene set database between 12mo Ctrl and 12mo sh*IRF7 *were plotted according to the difference between the ES values of the "1mo vs. 12mo" and the "12mo-Ctrl vs. 12mo-sh*IRF7*" microarray dataset (A). Genes with a significantly different expression (T-TEST, p Value<0.05) in 12mo sh*IRF7 *vs 12mo Ctrl MSC were functionally categorized based on the KEGG 2019 mouse algorithm (B). GSEA analysis for three distinct mitochondrial related gene sets from the Gene Ontology Consortium database confirmed the enrichment of mitochondrial genes in 12mo sh*IRF7 *MSC compared to controls (C).*

IRF7 inhibition restore mitochondrial function

According to the transcriptional data, 12mo shIRF7 cells showed a significantly higher number of mitochondria displaying more structured cristae compared to controls

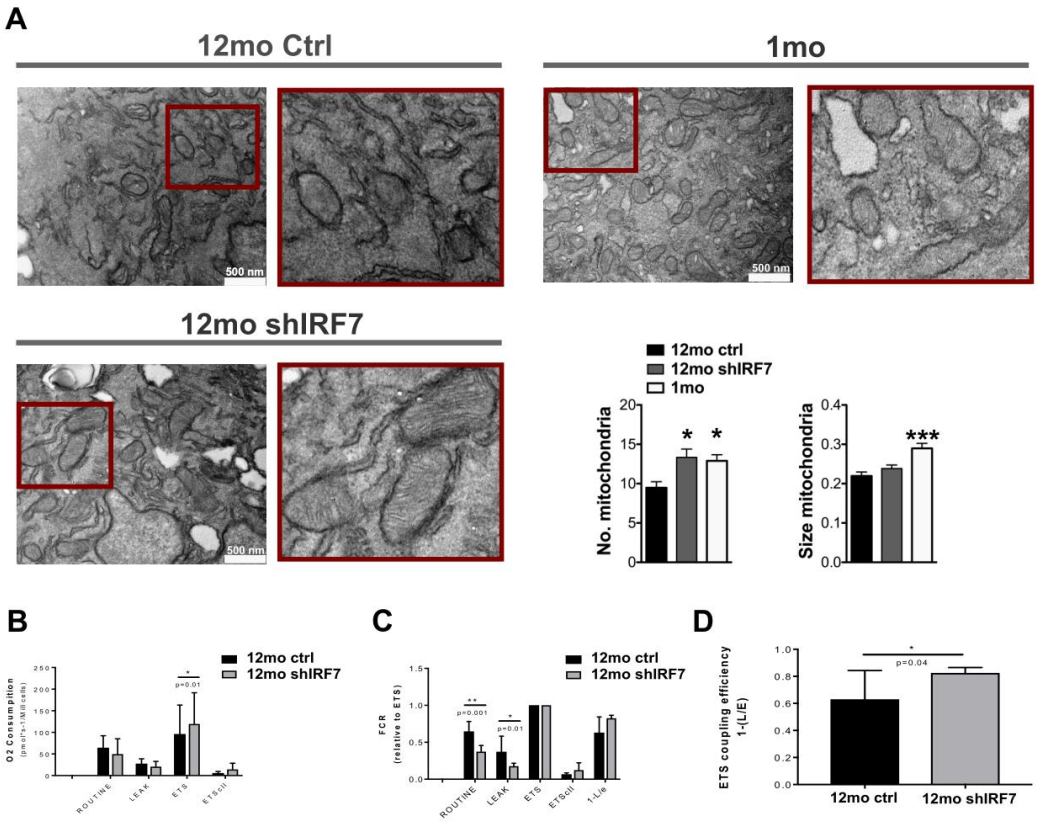

*Figure 15: Mitochondria in sh*IRF7 *were significantly more abundant and displayed more structured cristae (One way ANOVA, Dunett post-hoc *p<0.05 **p<0.01 ***p<0.0001 compared to 12mo ctrl) (**A**). Mitochondrial function was evaluated with high resolution respirometry in intact cells. Quantitative analysis of oxygen consumption in ROUTINE, LEAK and ETS respiratory (**B**). Data expressed relatively to ETS in the same respiratory states (**C**). ETS coupling efficiency expressed as 1-(L/E). (Data are reported as mean ±SD, n=5; ANOVA and paired t-Test; p<0.05) (**D**).*

(Figure 15**A**). To evaluate the effect of IRF7 depletion on mitochondrial function we compared in parallel oxygen consumption in various respiratory states of 12mo shIRF7 versus 12mo ctrl. In oxidative phosphorylation, the endergonic process of phosphorylation of ADP to ATP is coupled to the exergonic process of electron transfer to oxygen. Coupling is achieved through the proton pumps generating and utilizing the protonmotive force in a proton circuit across the inner mitochondrial membrane. This proton circuit is partially uncoupled by proton leaks. Intrinsic uncoupling under physiological conditions is a property of the inner mitochondrial membrane (proton leak). Cell respiration in vivo is regulated according to physiological activity, at ROUTINE activity. ROUTINE cell respiration can be inhibited by oligomycin intracellular non-saturating ADP levels in ROUTINE states of activity. When incubated for short experimental periods in a medium devoid of organic

substrates, the cells respire solely on endogenous substrates at the corresponding state of to a resting state, corresponding mainly to LEAK respiration, comparable to isolated mitochondria. Cells with standard or endogenous substrate supply can be activated by uncoupling to reveal the maximal uncoupled oxidative capacity (ETS). The ETS was significantly increased by 25% (p=0.02) in 12mo shIRF7 (Figure 15 **B, C and D**). Data normalized to ETS show that 12mo shIRF7 cells have reduced oxygen consumption in the basal ROUTINE (p=0.004) state as well in the dissipative LEAK state by ≃50% (p=0.02). Lower oxygen consumption in the ROUTINE and LEAK states is accompanied by an increase of the ETS coupling efficiency, expressed as 1-(L/E), by 32% (p=0.038). These data show that IRF7 inhibition significantly improves mitochondrial function.

IRF7 knock-down restores the intracellular amino acid pool.

The inhibition of IRF7 reverted partially the major metabolomic changes which occurred with aging in MSC (Figure 16).

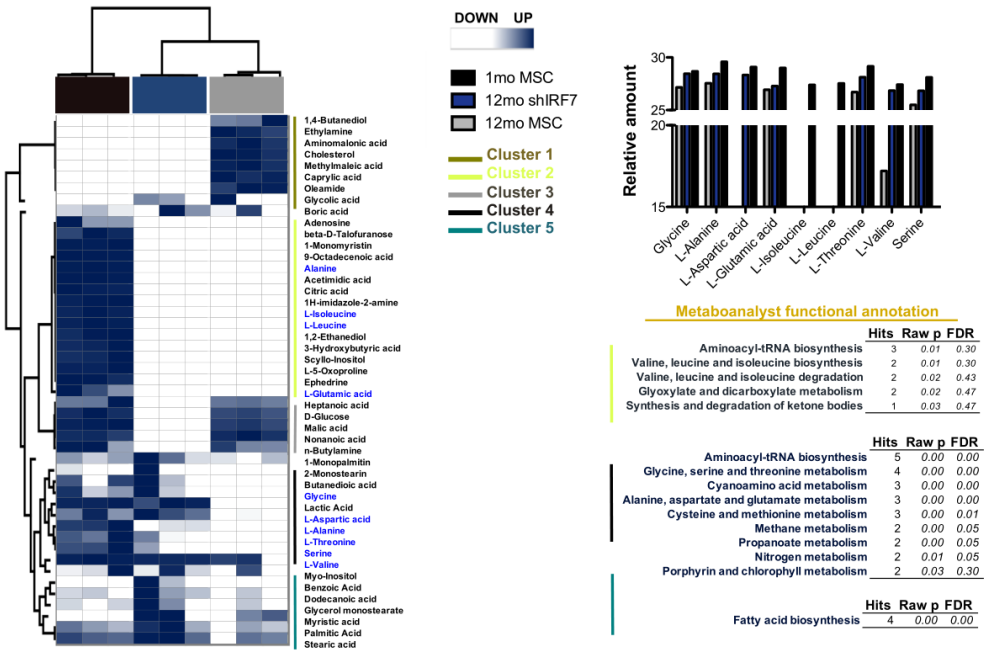

Figure 16: Unsupervised hierarchical clusterization of the metabolomic profile of 1mo, 12mo shIRF7 and 12mo-ctrl (scramble and empty vector) MSC allowed to identify 5 major clusters of metabolites. All amino acids reduced in aged cells were restored upon IRF7 knock-down, except leucine and isoleucine (right panel). Functional analysis of the metabolites comprised in the cluster identified in figure 6A show that 3 out of the 5 clusters were significantly enriched of functional annotation terms related to either amino-acid metabolism and translation (Cluster 2 and 4) or fatty acid metabolism (Cluster 5). Cluster 1 and 3 were not significantly classified into any functional category.

All the metabolite upregulated in 12mo compared 1mo MSC, which were attributable to an altered inflammatory and proteostasis phenotype (i.e. cholesterol, caprylic acid, amino malonic acid, nonanoic acid), resulted cleared in 12mo-shIRF7 MSC (*Cluster 1*). After IRF7 inhibitions, succinate was successfully restored (Cluster 4), but not the other TCA related intermediated, i.e. citrate and malate (Cluster 2).

Also, the amino acids depleted in 12mo compared to 1mo MSC (Figure 11**C**) were restored in 12mo shIRF7 MSC, except for the BCAAs leucine and isoleucine (*cluster 2 and 4*). Surprisingly, we did not find coordinated changes in the transcription of the genes involved in amino acid biosynthesis (Figure 17**A**) and degradation (Figure 17**B**). However, 12mo shIRF7 MSC showed the drastic enrichment of genes involved in BCAA degradation (Figure 17**C**). Genes involved in BCAAs degradation was found down-regulated in 12mo compared 1mo MSC (Figure 12 and Figure 13).

Moreover, we found a significant upregulation of the gene encoding for PP2Cm (*Ppm1K)* (Figure 17**C**), the mitochondrial localized enzyme which activates branched-chain alpha-ketoacid dehydrogenase (BCKDH) complex, the rate-limiting enzyme of the BCAA degradation pathway, and the loss of which has been reported to impair mitochondrial function, to increase oxidative stress, abnormal cardiac and neural development [86]. In addition, we found increased transcriptional levels of the Krupple-like factor 15 (*Klf15*) (Figure 17**C**) which has been previously shown to be a master inducer of BCAA degradation genes and to be crucial to prevent mitochondrial dysfunction and oxidative stress in hearth [42,87,88]. INTERFEROME analysis confirmed that genes involved in BCAA degradation pathway have been experimentally identified as ISGs and that they have been found to be mainly down-regulated upon IFN stimulation (Figure 17**D e E**).

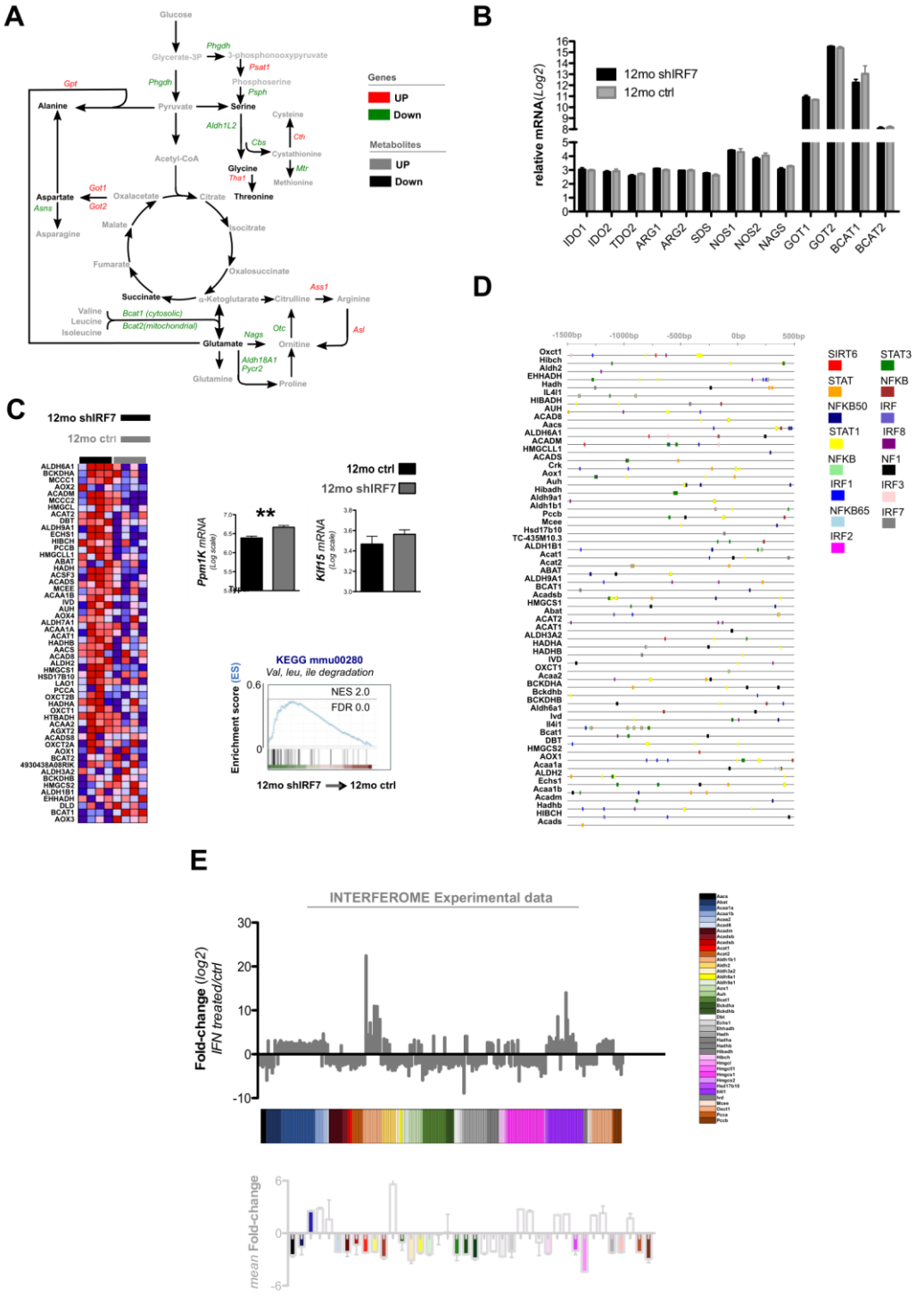

*Figure 17: Genes implicated in amino acid biosynthesis did not exhibit coordinated changes upon Irf7 knockdown (**A**). Genes encoding for the enzyme involved in amino acid degradation were not coordinately changed upon Irf7 knockdown (**B**). Genes involved in BCAA degradation pathways and their major regulators (such as Ppm1k and Klf15) were enriched upon IRF7 knockdown (**C**). Genes encoding for the enzyme involved in TCA cycles reported in Figure 6C were recognized as interferon stimulated genes (ISGs) according to INTERFEROME database and many IFN-related transcription factor motifs were identified within their promoter region (**D**). These gene are predicted to be downregulated upon IFNs treatment according to the INTERFEROME experimental data (**E**).*

INTERFEROME analysis revealed that all the TCA cycle genes upregulated in 12mo shIRF7 are ISGs and have been experimentally reported to be down-regulated by the IFNs (Figure 18**A and B**). Moreover, enhanced BCAAs degradation is strictly linked to increased Fatty Acid Oxidation (FAO) [89–91] and these two pathways share many common enzymes (Figure 18**C**). Consistently with this notion, we found a significant enrichment of the FAO genes 12mo in 12mo shIRF7 cells (Figure 18**C**).

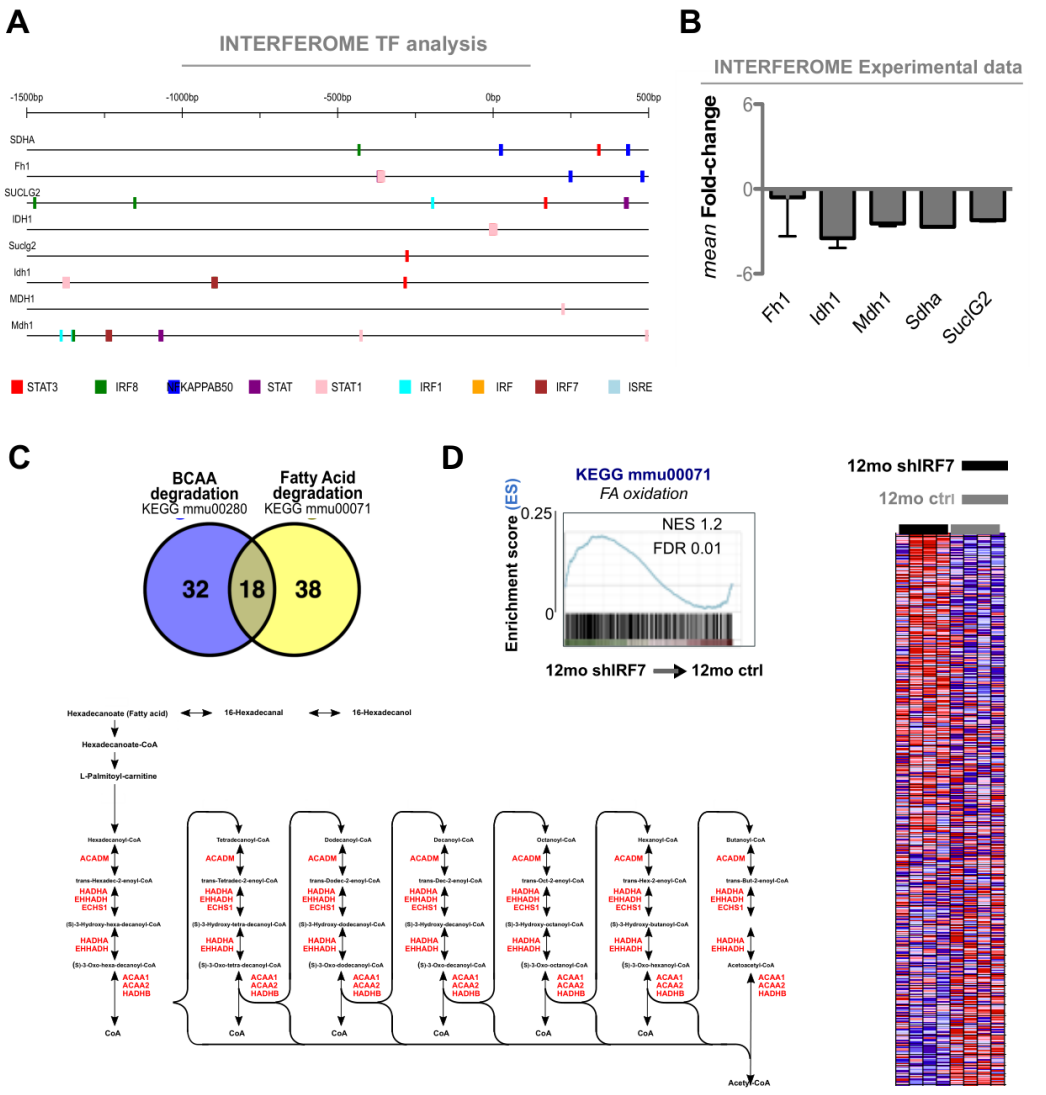

*Figure 18: Genes encoding for the enzymes involved in the Branched Chain amino acid (BCAA) degradation are identified as ISGs according to INTERFEROME database , display multiple IFN-related transcriptional motifs within their promoter region (**A**) and resulted to be mainly downregulated upon IFN treatment (**B**). BCAA degradation and Fatty Acid Oxidation (FAO) pathways share 18 genes in common (**C**). FAO related genes are upregulated upon IRF7 knock-down (**D**).*

This drives to speculate that the rescue of the amino acid pool after IRF7 inhibition relies on an increased BCAAs (leucine and isoleucine) degradation, which feeds TCA cycle (anaplerosis) to replenish the oxaloacetate as fast as it is diverted (cataplerosis)

towards the amino acid biosynthetic pathways (Figure 19). Consistently with this model, six out of eight genes encoding for the enzymes involved in the TCA cycle were upregulated in 12mo shIRF7 cells. The exceptions were *Succinate dehydrogenase* (*SdhA*), which converts succinate to fumarate, and *Citrate synthase* (*Cs*), which regenerate citrate from oxaloacetate to run a new cycle (Figure 19). The enzyme which catalyses the steps immediately upstream these two reactions were strongly upregulated. These were *Succinate CoA-ligase GDP forming beta-subunit* (*SuclG2, p=0.03*), which converts Succinyl-CoA to Succinate, and *Malate dehydrogenase 1* (*Mdh1, p=0.07*), which transforms malate to oxaloacetate. The fact that the enzymes upstream of succinate synthesis are up regulated and those downstream are down regulated, explains the abundance of succinate in 12mo shIRF7 MSC. This might be consistent with the enhanced OXPHOS function as succinate interacts directly with the mitochondrial electron transport chain through succinate dehydrogenase (SDH; succinate: ubiquinone oxidoreductase; mitochondrial complex II), that catalysis the oxidation of succinate to fumarate and the reduction of ubiquinone (UQ) to ubiquinol

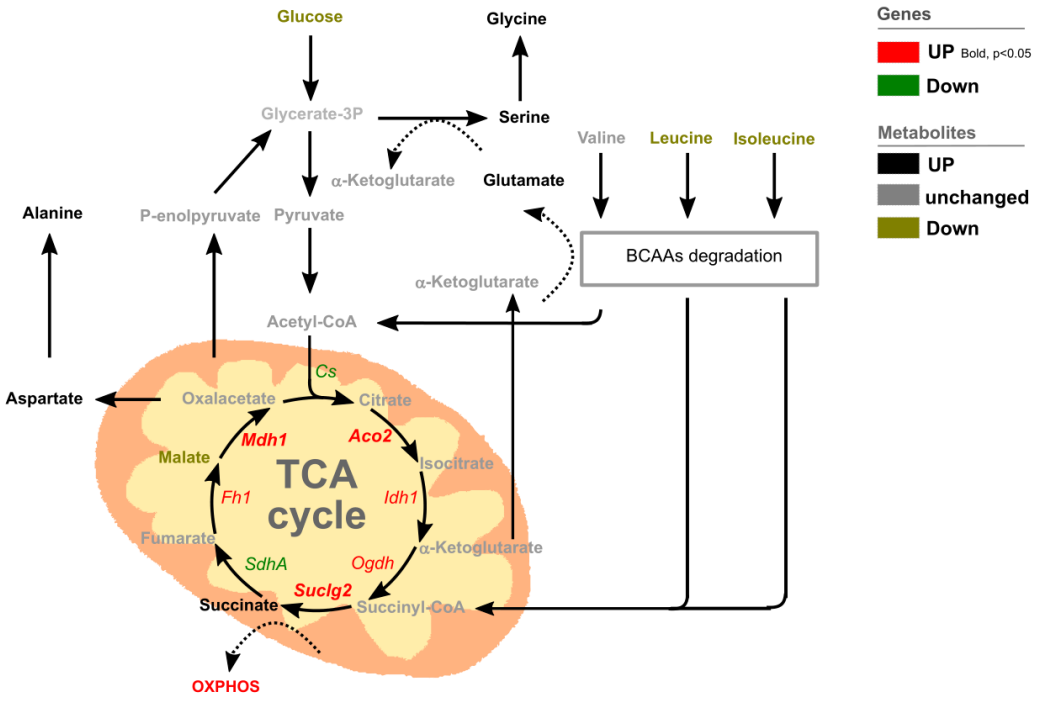

Figure 19: TCA cycle provides oxaloacetate, which serves as common precursor of aspartate, alanine, serine and glycine. Genes encoding for the enzyme which catalyzes the various steps of TCA cycle are significantly upregulated (red bold), non-significantly upregulated (red) or non-significantly down-regulated (green). BCAA degradation provides glutamate and feeds TCA cycle (C).

(UQH2), thereby linking the tricarboxylic acid (TCA) cycle and the electron transport system (ETS) and enabling a 'shortcut' route to ATP production via oxidative metabolism. In sharp contrast, despite the increase of Mdh and the decrease of Cs expression, the oxaloacetate did not change. This indicates that the enhanced rate of its generation makes oxaloacetate always available and this might favour the cataplerotic diversion towards extra-TCA cycle pathways likely to re-establishment of Aspartate, Alanine, Serine and Glycine.

To understand if the variations observed in the elements of these pathways modulate the activity of mitochondrial complexes in responses to specific substrates, we used permeabilized 12mo-shIRF7 and 12mo-Ctrl cells. The octanoyl-carnitine fatty acid, malate, glutamate and succinate were used as substrates to sustain ETF, complex I and complex II and ROUTINE, LEAK, OXPHOS and ET respiratory states were evaluated. Overall 12mo-shIRF7 cells didn't show significative changes in the rates of oxygen consumption compared to controls (Figure 20**A**). However analysis of flux control ratios (data expressed relatively to P_{OMGS}) indicated that there are significant differences in 12mo-IRF7 cells compared to controls ($F(7, 32)=68.22$ $p<0.0001$) and shows that maximal uncoupled mitochondrial capacity (ET_{OMGS}) is significantly higher in 12mo-shIRF7 compared to 12mo-Ctrl cells (+19% p=0.02) (Figure 20**B**). In addition investigating the effect of addition of glutamate (G) in the OXPHOS state, by using the control factor P_{OMG}-P_{OM}/P_{OMG}, we observed a remarkable stimulation in 12mo-shIRF7 compared to 12mo-ctrl cells (+80% p=0.02) (Figure 20**C**), suggesting that 12mo-shIRF7 cells are more sensitive to glutamate than controls.

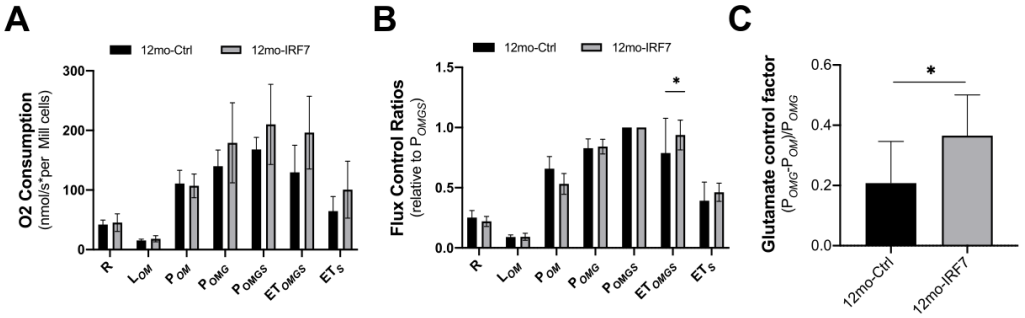

Figure 20: Quantitative analysis of the rates of oxygen consumption in ROUTINE (R), LEAK (L), OXPHOS (P) and ET (E) respiratory states in 12mo-Ctrl and 12mo-IRF7 permeabilized cells (G). Flux control ratios expressed relatively to POMGS in the ROUTINE (R), LEAK (L), OXPHOS (P) and ET (E) respiratory states in 12mo-Ctrl and 12mo-IRF7 permeabilized cells (H). Effect of addition of glutamate in 12mo-Ctrl and 12mo-IRF7 permeabilized cells evaluated using the control factor POMG-POM/POMG (I). (G,H, I - Data are reported as mean ±SD, n=5; Two-way ANOVA with Sidak's post-hoc correction (G, H) and paired t-Test; P<0.05 (I); p<0.05).

These data confirm the improvement of mitochondrial function and show that the electron-transport system may have different sensitivity for specific substrates.

Collectively, our data demonstrate an unprecedented role of IRF7 in leading the IFN-mediated inactivation with age of "core" longevity biologic functions, namely mitochondrial and amino acid biogenesis. These functions are crucial to maintain proper cell homeostasis over chronic or acute stress conditions and underly the beneficial effects of life-extending interventions such as dietary restriction. Since viruses are able to subvert these functions to meet their own bioenergetic and biosynthetic demand, IFN pathways have evolved to counteract viral infection thought the temporary shutdown of these functions. We show herein that aging induces the ectopic (i.e. in absence of viral infection) activation of IFN program which impairs mitochondrial and amino acid biogenesis (Figure 21). IRF7 knockdown restores mitochondrial function and amino acid biosynthesis, at least partially through the activation of BCAA and FA degradation pathways

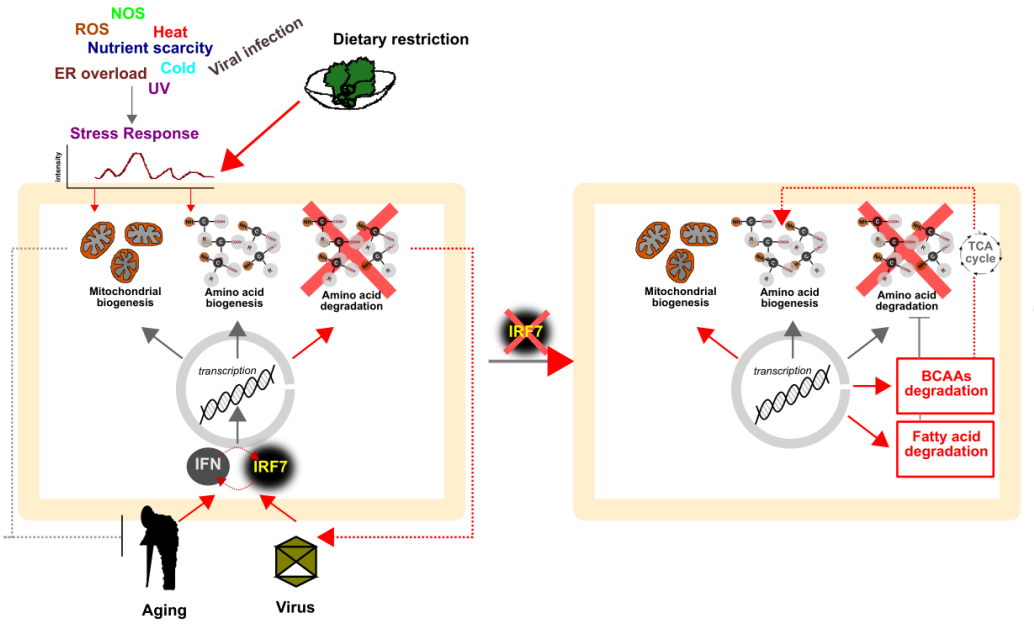

Figure 21: Model which shows aging as the ectopic activation of IRF7-IFN signaling pathway which impairs "core" longevity biological functions. Mitochondrial and amino acid biogenesis are the common outcomes of successful integrated stress response pathways and life-extending interventions such as dietary restriction. Virus are thought to stimulate integrated stress response too, with the aim of subverting the host bioenergetic and biosynthetic machinery for their replication. To prevent this effect cell have evolved IFN signaling pathways, which shut off these functions. Aging induces the ectopic activation of this process (in absence of real viral infection) with detrimental effects on the organism fitness and longevity. IRF7 inhibition restores mitochondrial biogenesis and rescue the amino acid pool likely though the activation of BCAA and FA degradation pathways which feed TCA cycle anaplerosis to support the amino acid biosynthetic pathway

Materials and Methods

Isolation of Adipose derived MSCs

The inguinal fat pads of FVB mice aged 1 (n=8) and 12 (n=8) months were surgically excised, weighed and processed to isolate the adipose-derived stromal cells, according to standard protocols[92]. Briefly, the extracellular matrix was digested with collagenase (1 mg/ml) and centrifuged to obtain a high-density pellet, the stromal vascular fraction (SVF). After centrifugation, the SVF cell number was determined using light microscopy, and the cells were plated at a concentration of 1×10^5 cells/cm^2 using DMEM medium (with high glucose concentration, GLUTAMAX I™, 10% FCS, 100 U/ml penicillin and 100 μg/ml streptomycin). After 2 to 3 weeks of culture, a homogeneous cell population was obtained. The cells were identified as MSCs on the basis of their immunophenotype. Specifically, the positivity of CD106 (VCAM1), CD73, CD29, CD44, CD90 and the lack of hematopoietic (antiCD45, CD14, CD11c, CD123 and CD34 monoclonal antibodies) and endothelial cell markers (with CD31 monoclonal antibody) were assessed by means of cytofluorimetric analysis.

Microarray Analyses

Whole-genome microarray analysis of MSC from differently aged mice was performed using the NimbleGen Gene Expression system. Briefly, total RNA was isolated from samples using the Qiagen RNeasy kit (Qiagen), following the manufacturer's instructions. RNA was used for cDNA synthesis followed by labelling of the cDNA with Cy3. The labelled cDNA samples were hybridized to *Mus musculus* 12x135K Array (Roche NimbleGen) which represents 44,170 mouse genes. The single colour NimbleGen arrays were scanned with GenePix 4400A Microarray Scanner. The data were extracted from scanned images using NimbleScan software and the Robust Multichip Average (RMA) algorithm was used to generate gene expression values. Hybridization, scanning and normalization of the data were performed as service by the Functional Genomic Centre of the University of Verona (Verona, Italy). Whole-genome microarray of shIRF7 silenced 12months-old MSC was performed as service by the UTSW Genomics Sequencing & Microarray Core Facility (Dallas, Texas, USA) on an Affymetrix platform (Clarion S Mouse Array).

GSEA

GSEA algorithm[72] sorts genes of the dataset by correlation with phenotypes and then it walks down the list increasing a running-sum statistic when it encounters a gene of the gene set of interest and decreasing it when it does not. The enrichment score (ES) is the maximum deviation from zero encountered in the random walk; it corresponds to a weighted Kolmogorov–Smirnov-like statistic. Normalized enrichment score (NES) for each gene set is calculated as the ratio between ES and the mean value of ES against all permutations of the default. It accounts for differences in gene set size and in correlations between gene sets and the expression dataset; therefore, NES can be used to compare analysis results across multiple gene sets.

Besides the enrichment scores, GSEA algorithm provides additional output parameters which identify the percentage of genes contributing to the enrichment result (leading edge analysis) and measure whether they are either concentrated on the extremities or spread through the ranked list of dataset genes. These are:

- Tags: the percentage of gene hits before (for positive ES) or after (for negative ES) the peak in the running enrichment score. This gives an indication of the percentage of genes contributing to the enrichment score.
- List: the percentage of genes in the ranked gene list before (for positive ES) or after (for negative ES) the peak in the running enrichment score. This gives an indication of where in the list the enrichment score is attained.
- Signal: the enrichment signal strength that combines the two previous statistics and the more gene set is spread throughout the list the more the signal strength decreases towards 0%.

Western Blotting

Immunoblots were performed according to standard procedures in RIPA buffer (150 mM NaCl, 10 mM Tris pH 7.5, 1% NP40, 1% Deoxycholate, 0.1% SDS) supplemented with phosphatase and protease inhibitors (SIGMA). Samples were resolved on Tris-glycine 4-20% gradient SDS-PAGE (BIO-RAD), blotted on Protran® membrane 0.2 μm (Whatman), incubated with the anti-IRF7 antibody [EPR4718] (Abcam #ab109255) and developed with ECL (Amersham).

Quantitative PCR

RNA was extracted using the Qiagen RNAeasy Plus mini kit. cDNA was generated by Superscript II (Invitrogen) and used with SYBR Green PCR master mix (Applied Biosystems) for real-time qPCR analysis. Assays were performed using an Applied Biosystems Step-One Real-Time PCR System.

Transmission electron microscopy

Samples were fixed with glutaraldehyde 2% in a Sorensen buffer pH 7.4 for 2 h, post-fixed in 1% osmium tetroxide in an aqueous solution for 2 h, dehydrated in graded concentrations of acetone, embedded in Epon-Araldite and cut with an Ultracut E Ultra-microtome (Reichert, Wien, Austria). At the end of the dehydrating process, samples were positioned in a multi-well grid for electron microscopy and observed using a TEM Morgagni 268D (FEI Philips). Quantification of mitochondrial size was performed using ImageJ software on the images taken at the same magnification from 20 randomly selected fields.

shRNA IRF7 lentiviral transduction

IRF7 was silenced in 12mo aged MSC by lentiviral transduction. 4 different shIRF7 into pLKO.1 vectors were used, named #1 (Dharmacon RMM3981-201795252), #2 (Dharmacon RMM3981-201798737), #3 (Dharmacon RMM3981-201788865) and #4 (Dharmacon RMM3981-201789942). Recombinant lentiviruses were generated in 293T cells transfected using the second-generation packaging vectors psPAX2 (Addgene#12260) and pMD2.G (Addgene#12259) using Lentifectin transfection reagent (ABM Good). Stably shIRF7 cells were selected with 1mg/mL Puromycin. 12mo MSC transduced with Empty (Addgene#10878) and shRNA scramble pLKO.1 (Addgene#1864) vectors were used as controls.

Metabolomic Analysis

Cells were trypsinized, washed with PBS solution and centrifuged. Supernatants were removed, and cells were resuspended in PBS. Aliquots containing $1x10^6$ of cells were used for the metabolite extraction. Metabolites were extracted using 760 µl of a precooled MeOH-Water mixture (1:0.9, v/v). Extracts were vortexed until complete dissolution of the pellet and 400 µL of ice-cold chloroform were added. Cells extracts were then homogenized with cell disrupter at 30 Hz for 10 min and centrifuged at

2200 g for 5 min at 4 °C. After layer separation, the polar and the nonpolar fractions were transferred to new precooled tubes[84]. The aliquots were then evaporated to dryness using a nitrogen flow and stored at 80 °C until analysis. Hexadecanoic acid as internal standard was added to the dried extract: the samples were first oximated by adding 30 µL of methoxyamine hydrochloride solution in pyridine (20 mg/mL), mixed in a vortex mixer and subsequently shaken for 90 min at 30 °C. Afterward, 30 µL of N,O-Bis(trimetylsilyl)trifluoroacetamide (BSTFA) with 1% trimethylchlorosilane (TMCS) were added and the derivatization was performed at 70 °C for 60 minutes prior to GC-MS analysis. An alkane standard mixture (C8-C20) was added as internal standard.

Gas chromatography–time of flight mass spectrometry (GC-TOF/MS) was performed using the Agilent 7890B GC (Agilent Technologies, USA) and Pegasus (BT) TOF-MS system (Leco Corporation, USA) equipped with an Rxi–5ms column (30m×0.25mm×0.25µm, RESTEK, USA), stationary phase 5% diphenyl-95% dimethyl polysiloxane. High-purity helium (99.999%) was used as the carrier gas at a flow rate of 1.20 mL/min^{-1}. Samples were injected in splitless mode at 250°C. The chromatographic conditions were: initial temperature 70°C, 2-minute isothermal, 6°C/min up to 160°C, 10°C/min up to 240°C, 20°C/min up to 300°C, 6 minutes isothermal. MS parameters: electron impact ionization source temperature (EI, 70 eV) was set at 250°C; scan range 40/630 m/z, with an extraction frequency of 30 kHz. The chromatograms were acquired in TIC (total ion current) mode. Mass spectral assignment was performed using the ChromaTOF BT software (Leco Corporation, USA) by matching with NIST MS Search 2.2. Libraries implemented with the MoNa Fiehns Libraries. Statistical and pathway studies were carried out by MetaboAnalyst 4.0 tool.

Mitochondrial respiration

To analyze mitochondrial respiration in MSCs cells (transfected with Ctrl or shIRF7 vectors) we used an Oxygraph-2K (Oroboros Instruments, Innsbruck). Instrumental and chemical background fluxes were opportunely calibrated as a function of oxygen concentration using DatLab software (Oroboros Instruments. All the measures were performed comparing cells expressing containing the two constructs in parallel in the

same experiment. Mitochondrial respiration was evaluated both in intact and permeabilized cells.

Intact cells. Cells resuspended in DMEM (250.000/ml) were analyzed applying a coupling control protocol[93] to determine the rate of oxygen consumption in the various respiratory states: ROUTINE, LEAK respiration, ETS (Electron Transfer System) capacity and ROX (Residual Oxygen Consumption) (Gnaiger et al., 2019). After stabilization of the rate of oxygen consumption in the ROUTINE respiration with addition of pyruvate and malate (5 mM and 2 mM, respectively) (Sigma Aldrich), the ATP-synthase inhibitor oligomycin (Omy, 2 μg/mL) (Sigma Aldrich) was added to obtain a measure of LEAK respiration, followed by titration of CCCP to maximum oxygen flux (ETS capacity). Finally, Rotenone (Rot) and Antimycin A (Ama) were added to inhibit specifically complex I and III respectively and obtain residual oxygen consumption (ROX).

Permeabilized cells. The respiration of permeabilized cells was determined using a modified substrate-uncoupler-inhibitor titration (SUIT) protocol (Pesta and Gnaiger, 2012). To investigate the contribution of different mitochondrial complexes (I-IV) to respiratory capacity, cells were permeabilized with the mild detergent digitonin (12 $\mu g/10^{-6}$ cells, Sigma Aldrich). This concentration was evaluated in preliminary experiments as suitable to achieve full permeabilization of cells allowing the access of substrates and ADP to mitochondria without compromising mitochondrial function. To evaluate the contribute of fatty acids to mitochondrial activity Octanoylcarnitine and Malate (OM; 0.8 mM and 2 mM respectively) were added in the ROUTINE state (R_{OM}). Following permeabilization with digitonin, the OXHPOS capacity (P_{OM}) was measured by adding ADP (5mM, Sigma Aldrich) and successively Glutamate (G; 10mM), were used to determine complex I activity (P_{OMG}). To activate complex II, the succinate (P_{OMGS}) was added (10 mM, Sigma Aldrich). The presence of all these substrates (OMGS) allows detecting the respiratory activity of linked complexes I, ETF and complex II. The contribution of complexes III and IV to respiratory activity is always present, although they were not stimulated by the addition of specific substrates.

To analyze the electron transfer system (ET_{OMGS}) capacity, steps titrations with the uncoupler CCCP (0.5 μM steps; Sigma Aldrich) were performed. Rot and Ama (2 and 2.5 μM respectively; Sigma Aldrich) were added to inhibit complex I (ET_S) and III

determining residual oxygen consumption (ROX). Raw data were analyzed with DatLab 6 Program (Oroboros Instruments).

Discussion

Aging is a multifactorial process which brings about multiple physiological alterations and geriatric syndromes such as metabolic syndrome, frailty, sarcopenia, chronic obstructive pulmonary disease, cancer, neurodegenerative diseases and many others. As such, according to the "geroscience hypothesis", the discovery of novel therapeutic strategies capable to dampen the general process of aging is a more straightforward challenge than fighting each of these specific age-related disorders [88].The detrimental effects of aging manifests early throughout the course of adult life [3,5–7,23,24,50,94] and their molecular determinants has been recently supposed to follow a non-linear progression rate, with a boost at middle-age (midlife switch)[5]. Many decades of studies have contributed to dissect pathways that are involved in aging and aging-related diseases [50]. However, paradigms capable to explain the causal connection between them and their hierarchical contribution to the aging phenotype are currently subject of intense debate with no conclusion drawn yet [4].

We show herein that aging matches with a general transcriptional derangement. Consistent with previous studies that describe an inhomogeneous and chaotic reorganization of transcription with age [24,26–32,35,46,95], we found that old phenotype is characterized by a large enrichment of gene sets that not fully satisfy cell functional program. Approaching to midlife cells start to translate genes that aren't really necessary and this lead to a chaotic state that is hard to resolve.

We showed that transcriptional deregulation is linked to the activation of INF signalling. Chronic inflammation, inflammaging, is a common trait of aging, and occurs not only at systemic level, but also in a cell-autonomous way triggering innate defence mechanism of cells, which do not necessarily belong to the immune compartment [96]. Our results point out IRF7 as the main driver of INF signalling with age. Moreover, IRF7 silencing is sufficient condition for, not only INF signalling inhibition, but also to widely revert transcriptional alterations.

The role of IRF7 as a regulator of immune cell function has been extensively investigated by thousands of studies. In sharp contrast, its expression and function in non-immune cells remains unexplored. Our data demonstrates that the role of IRF7 extends beyond the protection against external intruders and its gain of function may indeed represent an intrinsic paradigm of the degeneration over the adulthood. This supports general notion that aging underlies the "hyperfunction" of processes that are

useful in youth but may turn detrimental in adults (9). This is in line with recent studies that have implicated IRF7 and interferon signalling in physiological or pathological processes that hallmark aging related diseases. Puthia et al. [97] showed that IRF7 inhibition prevents destructive innate immunity and it may be a target for non-antibiotic therapy of bacterial infections. Wang et al. [98] showed that Interferon regulatory factor 7 deficiency prevents diet-induced obesity and insulin resistance, two pathological conditions that are strictly associated with aging. Baruch et al. [68] showed that IFN-I signalling increases with aging in the choroid plexus and its pharmacological inhibition prevents the aging-associated cognitive impairment.

Along with the increase of INF signalling, our aging model has highlighted a marked decrease in mitochondrial function and in amino acid biogenesis, which are common outcomes of the ancient evolutionary conserved programs referred to as integrated stress response (ISR) [51,52]. Mitochondrial function is fundamental to maintain metabolic homeostasis [99]. Homeostasis is the state of equilibrium that guarantees the optimal functioning for an organism. During lifetime homeostasis is continuously adjusted to face stress or stimuli. To fully fit changes the organism's homeostasis passes through alternative stable states regulated, both at systemic and intracellular level, by multiple set points. As consequence, homeostatic systems are vulnerable to dysregulation because they are designed to be adjustable [63]. Homeostasis during time of stress is preserved by complex inter-play of many critical stress-response pathways specific for each cellular sub-compartment, these responses are interconnected and interdependent to cellular fitness [100]. At cellular level, integrated stress response pathways act constitutively as quality control mechanism. At the same time, these pathways are massively invoked to respond to multiple acute or chronic stress conditions such as nutrient deprivation, oxidative environment, proteotoxic stress, endoplasmic reticulum (ER) overload, viral infection, etc. [48,51]. Mitochondria are both targets and master regulators of these stress response programs. Beyond their bioenergetic role, mitochondria have evolved as signalling organelles which instruct nuclear transcription, cytosolic protein translation and metabolic rewiring to coordinate the cellular adaptation to environmental changes [48,58,101–103]. Briefly, the activation of mitochondrial and amino acid biogenesis by integrated stress response pathways is achieved through a programmed switch to the preferential translation of specific mRNA, endowed with alternative (cap-independent) open reading frames,

over a global reduction of general translation of cap-dependent mRNAs [48–51,53,55,57]. Stress-selected mRNAs encodes for components and master regulators of mitochondrial and amino acid biogenesis [50,51,55,56]. Viral infection is commonly enlisted among the major inducers of the stress response [52]. However, the outcome of the host response to viral infection is paradoxical. Since viral mRNAs translation is driven by non-canonical ORFs, common stress response pathways are subverted by the virus as a subtitle strategy to usurp the host bioenergetic and translation machinery [69]. On the other hand, cells have also evolved Interferon(IFN)-signalling to counteract the viral infection [65,66]. IFNs instructs the transcription of thousands of genes (Interferon stimulated genes, ISGs), which prime systemic innate immunity and lead cell-autonomous pathways of self-defence [65,66]. However, the anti-viral function of these genes and their impact on cell homeostasis are only partially understood [104]. Chronic inflammation is a common accomplice of the disease of homeostasis [63]. Inflammation comes as a defence when the mechanisms to restore homeostasis are insufficient. So, the inflammatory response, that have higher physiological priority, achieve the control by overriding or suppressing homeostatic set point [63]. However, if inflammation enforce and propagate changes that are detrimental, chronic pathological states can result. The system become locked in a state of a chronic inflammation that fails to resolve and may, in turn, account for the persistence of chronic diseases [105]. Rise of inflammation during aging controverts its original purpose. When properly activated to counteract infection, inflammation provides beneficial condition which overweighs possible non-adaptive detrimental effect. But in aging, the balance in this trade-off is shifted, making a non-adaptive trait an unavoidable detrimental consequence [61]. The pathological inflammatory state is assumed to have a beneficial counterpart, but, in case of aging, it seems caused by a homeostasis imbalance of one or more physiological systems, that are not functionally linked to host defences or repair systems. Probably, it rises from an adaptative mechanism to restoring homeostasis, likely the response to viral infection, but locked in a state impossible to resolve.

Mitochondria play active roles in driving homeostatic pathways as upon acute stress conditions they may generate retrograde stress signals which instruct the nucleus to selectively reactivate the transcription of genes encoding for mitochondrial components and mitochondrial translational machinery [48,52,58]. Hence, maintenance of proper mitochondrial activity is a priority challenge for cells and organs, which should

be accomplished over stress-induced adaptive rearrangements [51,52]. Mitochondrial number, structure and function was completely restored upon IRF7 inhibition.

We show that the increased expression of IRF7 leads the ectopic activation of cell-autonomous pathways of self-defence which dampens mitochondrial and amino acid biogenesis, two biological functions that are crucial for cell homeostasis and underly the beneficial effects of well-established age-preventing and life-extending interventions such as dietary restriction [49,50].

IRF7 silencing reverts aging-induced IFN activation and partially restore mitochondrial function and amino acid biogenesis. Although IRF/ inhibition did not reverted the aging-related transcriptional changes of genes involved in aa biosynthesis and degeneration, the intracellular aa pool was restored except for leucine and isoleucine. This drive us to speculate that despite the suppression of INF signalling, After IRF7 inhibition, the intracellular pool of amino acid was restored, except for leucine and isoleucine, but we did not find coordinated changes in the transcription of the genes involved in amino acid biosynthesis and degradation. This drive us to speculate that after suppression of IFN signalling, despite an intrinsic impossibility to return to the young steady state, cells are trying to re-establish the amino acidic pool depleted by aging through BCAAs degradation. , which feeds TCA cycle and represent an alternative way to support amino acid biosynthesis. Our data might suggest that shutting down inflammation the regulatory apparatus of the cell can re-establish its normal function, take the control and implement mechanisms that guarantee the homeostasis (health).

Our results reveal IRF7 to be a major causal link between two long recognized hallmarks of aging, which are metabolic dysfunctions and low-grade, chronic inflammatory state referred to as "Inflammaging" [1]. Previous studies in recent years have explored the reciprocal causal connections between mitochondria and inflammation, and their possible role in aging. Recent studies have shown that mitochondrial disruption may trigger inflammatory reactions [18,106,107], while pro-inflammatory mediators may contribute, in turn, to alter mitochondrial activity [94]. However, mechanisms modelled in these studies implicate the systemic recruitment of immune cells (neutrophils, macrophages) [107,108], circulating pro-inflammatory cytokines (TNF-alpha, IL6, IL1) [94,109], cell debris [110] or DNA damaging chemical mediators (ROS, NOS) [106,111] and have ultimately contributed to establish the prevailing notion that the

aging-related deterioration of tissue function and mitochondrial integrity relies on a complex bi-directional interaction between systemic immunity and tissue resident cells. We provide herein an additional, cell-intrinsic perspective, which envisions the age-related mitochondrial dysfunction of non-immune cells as the consequence of "cell-autonomous" alterations of immunity-related signalling pathways. IRF7 functions as the molecular trigger of these pathways with aging. Whether the increased expression of IRF7 with age is primed by extrinsic or intrinsic factors is not clear. Nevertheless, its impact on the transcription of immune and mitochondrial genes is cell-autonomous, as it persists in cultured cells over multiple passages, and reversible, thus ruling out the involvement of genetic damages eventually induced by extracellular mediators such as ROS and NOS, previously implicated in connecting inflammatory response with mitochondrial integrity.

According to these reports our results suggest IRF7 as an ideal target for the development of therapies which are potentially effective against multiple and intersecting aspects of aging phenotype.

Bibliography

1. Franceschi, C. & Campisi, J. Chronic Inflammation (Inflammaging) and Its Potential Contribution to Age-Associated Diseases. *J Gerontol A Biol Sci Med Sci* **69**, S4–S9 (2014).
2. Shaw, A. C., Goldstein, D. R. & Montgomery, R. R. Age-dependent dysregulation of innate immunity. *Nat Rev Immunol* **13**, 875–887 (2013).
3. D'Antona, G. *et al.* Branched-Chain Amino Acid Supplementation Promotes Survival and Supports Cardiac and Skeletal Muscle Mitochondrial Biogenesis in Middle-Aged Mice. *Cell Metabolism* **12**, 362–372 (2010).
4. Shoji, H., Takao, K., Hattori, S. & Miyakawa, T. Age-related changes in behavior in C57BL/6J mice from young adulthood to middle age. *Mol Brain* **9**, 11 (2016).
5. Mori, M. A. *et al.* Role of MicroRNA Processing in Adipose Tissue in Stress Defense and Longevity. *Cell Metabolism* **16**, 336–347 (2012).
6. Mori, M. A. *et al.* Altered miRNA processing disrupts brown/white adipocyte determination and associates with lipodystrophy. *J. Clin. Invest.* **124**, 3339–3351 (2014).
7. Berry, D. C. *et al.* Cellular Aging Contributes to Failure of Cold-Induced Beige Adipocyte Formation in Old Mice and Humans. *Cell Metabolism* **25**, 166–181 (2017).
8. Correia-Melo, C. *et al.* Mitochondria are required for pro-ageing features of the senescent phenotype. *EMBO J* **35**, 724–742 (2016).
9. Manaye, K. F. *et al.* Age-related loss of noradrenergic neurons in the brains of triple transgenic mice. *Age (Dordr)* **35**, 139–147 (2013).
10. Wu, L. E., Gomes, A. P. & Sinclair, D. A. Geroncogenesis: metabolic changes during aging as a driver of tumorigenesis. *Cancer Cell* **25**, 12–19 (2014).
11. Franceschi, C. *et al.* The Continuum of Aging and Age-Related Diseases: Common Mechanisms but Different Rates. *Front Med (Lausanne)* **5**, 61 (2018).

12. The challenge of ageing population to be tackled with the first Horizon Prize for Social Innovation - News Alert - Research & Innovation - European Commission. https://ec.europa.eu/research/index.cfm?pg=newsalert&year=2015&na=na-221015.
13. López-Otín, C., Blasco, M. A., Partridge, L., Serrano, M. & Kroemer, G. The Hallmarks of Aging. *Cell* **153**, 1194–1217 (2013).
14. Harman, D. Free radical theory of aging: The "free radical" diseases. *AGE* **7**, 111–131 (1984).
15. Liguori, I. *et al.* Oxidative stress, aging, and diseases. *Clin Interv Aging* **13**, 757–772 (2018).
16. Mills, E. L., Kelly, B. & O'Neill, L. A. J. Mitochondria are the powerhouses of immunity. *Nat Immunol* **18**, 488–498 (2017).
17. Doonan, R. *et al.* Against the oxidative damage theory of aging: superoxide dismutases protect against oxidative stress but have little or no effect on life span in Caenorhabditis elegans. *Genes Dev.* **22**, 3236–3241 (2008).
18. Zhang, Y. *et al.* Mice Deficient in Both Mn Superoxide Dismutase and Glutathione Peroxidase-1 Have Increased Oxidative Damage and a Greater Incidence of Pathology but No Reduction in Longevity. *J Gerontol A Biol Sci Med Sci* **64A**, 1212–1220 (2009).
19. Blagosklonny, M. V. Aging: ROS or TOR. *Cell Cycle* **7**, 3344–3354 (2008).
20. Blagosklonny, M. V. Paradoxes of Aging. *Cell Cycle* **6**, 2997–3003 (2007).
21. Blagosklonny, M. V. Aging is not programmed. *Cell Cycle* **12**, 3736–3742 (2013).
22. Blagosklonny, M. V. Aging and Immortality: Quasi-Programmed Senescence and Its Pharmacologic Inhibition. *Cell Cycle* **5**, 2087–2102 (2006).
23. Gems, D. & Partridge, L. Genetics of Longevity in Model Organisms: Debates and Paradigm Shifts. *Annual Review of Physiology* **75**, 621–644 (2013).
24. Timmons, J. A. *et al.* Longevity-related molecular pathways are subject to midlife "switch" in humans. *Aging Cell* **18**, e12970 (2019).

25. Martinez-Jimenez, C. P. *et al.* Aging increases cell-to-cell transcriptional variability upon immune stimulation. *Science* **355**, 1433–1436 (2017).

26. Bahar, R. *et al.* Increased cell-to-cell variation in gene expression in ageing mouse heart. *Nature* **441**, 1011–1014 (2006).

27. Cheung, P. *et al.* Single-Cell Chromatin Modification Profiling Reveals Increased Epigenetic Variations with Aging. *Cell* **173**, 1385-1397.e14 (2018).

28. Davie, K. *et al.* A Single-Cell Transcriptome Atlas of the Aging Drosophila Brain. *Cell* **174**, 982-998.e20 (2018).

29. Enge, M. *et al.* Single-Cell Analysis of Human Pancreas Reveals Transcriptional Signatures of Aging and Somatic Mutation Patterns. *Cell* **171**, 321-330.e14 (2017).

30. Somel, M., Khaitovich, P., Bahn, S., Pääbo, S. & Lachmann, M. Gene expression becomes heterogeneous with age. *Current Biology* **16**, R359–R360 (2006).

31. Rangaraju, S. *et al.* Suppression of transcriptional drift extends C. elegans lifespan by postponing the onset of mortality. *eLife* **4**, e08833 (2015).

32. Southworth, L. K., Owen, A. B. & Kim, S. K. Aging Mice Show a Decreasing Correlation of Gene Expression within Genetic Modules. *PLOS Genetics* **5**, e1000776 (2009).

33. Arias, A. M. & Hayward, P. Filtering transcriptional noise during development: concepts and mechanisms. *Nature Reviews Genetics* **7**, 34–44 (2006).

34. Elowitz, M. B., Levine, A. J., Siggia, E. D. & Swain, P. S. Stochastic Gene Expression in a Single Cell. *Science* **297**, 1183–1186 (2002).

35. Sanchez, A., Choubey, S. & Kondev, J. Regulation of Noise in Gene Expression. *Annual Review of Biophysics* **42**, 469–491 (2013).

36. Fraser, H. B., Hirsh, A. E., Giaever, G., Kumm, J. & Eisen, M. B. Noise Minimization in Eukaryotic Gene Expression. *PLOS Biology* **2**, e137 (2004).

37. Thattai, M. & Oudenaarden, A. van. Intrinsic noise in gene regulatory networks. *PNAS* **98**, 8614–8619 (2001).

38. Benayoun, B. A. *et al.* Remodeling of epigenome and transcriptome landscapes with aging in mice reveals widespread induction of inflammatory responses. *Genome Res.* (2019) doi:10.1101/gr.240093.118.

39. De Cecco, M. *et al.* L1 drives IFN in senescent cells and promotes age-associated inflammation. *Nature* **566**, 73–78 (2019).

40. McDonnell, E. *et al.* Lipids Reprogram Metabolism to Become a Major Carbon Source for Histone Acetylation. *Cell Reports* **17**, 1463–1472 (2016).

41. Peleg, S., Feller, C., Ladurner, A. G. & Imhof, A. The Metabolic Impact on Histone Acetylation and Transcription in Ageing. *Trends in Biochemical Sciences* **41**, 700–711 (2016).

42. Sun, N., Youle, R. J. & Finkel, T. The Mitochondrial Basis of Aging. *Mol. Cell* **61**, 654–666 (2016).

43. Wallace, D. C. A mitochondrial paradigm of metabolic and degenerative diseases, aging, and cancer: a dawn for evolutionary medicine. *Annu. Rev. Genet.* **39**, 359–407 (2005).

44. Green, D. R., Galluzzi, L. & Kroemer, G. Mitochondria and the Autophagy–Inflammation–Cell Death Axis in Organismal Aging. *Science* **333**, 1109–1112 (2011).

45. Ramadasan-Nair, R. *et al.* Mitochondrial Alterations and Oxidative Stress in an Acute Transient Mouse Model of Muscle Degeneration. *J Biol Chem* **289**, 485–509 (2014).

46. McCarroll, S. A. *et al.* Comparing genomic expression patterns across species identifies shared transcriptional profile in aging. *Nat Genet* **36**, 197–204 (2004).

47. Peleg, S. *et al.* Life span extension by targeting a link between metabolism and histone acetylation in Drosophila. *EMBO reports* **17**, 455–469 (2016).

48. Quirós, P. M. *et al.* Multi-omics analysis identifies ATF4 as a key regulator of the mitochondrial stress response in mammals. *J Cell Biol* **216**, 2027–2045 (2017).

49. Steffen, K. K. & Dillin, A. A Ribosomal Perspective on Proteostasis and Aging. *Cell Metabolism* **23**, 1004–1012 (2016).

50. Zid, B. M. *et al.* 4E-BP extends lifespan upon dietary restriction by enhancing mitochondrial activity in Drosophila. *Cell* **139**, 149–160 (2009).

51. Harding, H. P. *et al.* An Integrated Stress Response Regulates Amino Acid Metabolism and Resistance to Oxidative Stress. *Molecular Cell* **11**, 619–633 (2003).

52. Pakos-Zebrucka, K. *et al.* The integrated stress response. *EMBO reports* **17**, 1374–1395 (2016).

53. Higuchi-Sanabria, R., Frankino, P. A., Paul, J. W., Tronnes, S. U. & Dillin, A. A Futile Battle? Protein Quality Control and the Stress of Aging. *Developmental Cell* **44**, 139–163 (2018).

54. Lu, G. *et al.* Protein phosphatase 2Cm is a critical regulator of branched-chain amino acid catabolism in mice and cultured cells. *J. Clin. Invest.* **119**, 1678–1687 (2009).

55. Lu, P. D., Harding, H. P. & Ron, D. Translation reinitiation at alternative open reading frames regulates gene expression in an integrated stress response. *The Journal of Cell Biology* **167**, 27–33 (2004).

56. Torrent, M., Chalancon, G., Groot, N. S. de, Wuster, A. & Babu, M. M. Cells alter their tRNA abundance to selectively regulate protein synthesis during stress conditions. *Sci. Signal.* **11**, eaat6409 (2018).

57. Tuller, T. *et al.* An Evolutionarily Conserved Mechanism for Controlling the Efficiency of Protein Translation. *Cell* **141**, 344–354 (2010).

58. Cardamone, M. D. *et al.* Mitochondrial Retrograde Signaling in Mammals Is Mediated by the Transcriptional Cofactor GPS2 via Direct Mitochondria-to-Nucleus Translocation. *Molecular Cell* **69**, 757-772.e7 (2018).

59. Houtkooper, R. H. *et al.* Mitonuclear protein imbalance as a conserved longevity mechanism. *Nature* **497**, 451–457 (2013).

60. Weinberg, S. E., Sena, L. A. & Chandel, N. S. Mitochondria in the Regulation of Innate and Adaptive Immunity. *Immunity* **42**, 406–417 (2015).

61. Medzhitov, R. Origin and physiological roles of inflammation. *Nature* **454**, 428–435 (2008).

62. Franceschi, C. *et al.* Inflamm-aging: An Evolutionary Perspective on Immunosenescence. *Annals of the New York Academy of Sciences* **908**, 244–254 (2000).

63. Kotas, M. E. & Medzhitov, R. Homeostasis, Inflammation, and Disease Susceptibility. *Cell* **160**, 816–827 (2015).

64. Sanada, F. *et al.* Source of Chronic Inflammation in Aging. *Front Cardiovasc Med* **5**, (2018).

65. Randow, F., MacMicking, J. D. & James, L. C. Cellular Self-Defense: How Cell-Autonomous Immunity Protects Against Pathogens. *Science* **340**, 701–706 (2013).

66. MacMicking, J. D. Interferon-inducible effector mechanisms in cell-autonomous immunity. *Nat Rev Immunol* **12**, 367–382 (2012).

67. Zhao, G.-N., Jiang, D.-S. & Li, H. Interferon regulatory factors: at the crossroads of immunity, metabolism, and disease. *Biochim. Biophys. Acta* **1852**, 365–378 (2015).

68. Baruch, K. *et al.* Aging. Aging-induced type I interferon response at the choroid plexus negatively affects brain function. *Science* **346**, 89–93 (2014).

69. Walsh, D. & Mohr, I. Viral subversion of the host protein synthesis machinery. *Nat Rev Microbiol* **9**, 860–875 (2011).

70. Raniga, K. & Liang, C. Interferons: reprogramming the metabolic network against viral infection. *Viruses* **10**, 36 (2018).

71. Zhang, W. *et al.* Aging stem cells. A Werner syndrome stem cell model unveils heterochromatin alterations as a driver of human aging. *Science* **348**, 1160–1163 (2015).

72. Subramanian, A. *et al.* Gene set enrichment analysis: a knowledge-based approach for interpreting genome-wide expression profiles. *Proceedings of the National Academy of Sciences* **102**, 15545–15550 (2005).

73. GSEA. http://software.broadinstitute.org/gsea/index.jsp.

74. Ashburner, M. *et al.* Gene ontology: tool for the unification of biology. The Gene Ontology Consortium. *Nat. Genet.* **25**, 25–29 (2000).

75. Expansion of the Gene Ontology knowledgebase and resources. *Nucleic Acids Res* **45**, D331–D338 (2017).

76. Rusinova, I. *et al.* Interferome v2.0: an updated database of annotated interferon-regulated genes. *Nucleic Acids Res.* **41**, D1040-1046 (2013).

77. York, A. G. *et al.* Limiting Cholesterol Biosynthetic Flux Spontaneously Engages Type I IFN Signaling. *Cell* **163**, 1716–1729 (2015).

78. Wang, J. *et al.* Caprylic acid and nonanoic acid upregulate endogenous host defense peptides to enhance intestinal epithelial immunological barrier function via histone deacetylase inhibition. *Int. Immunopharmacol.* **65**, 303–311 (2018).

79. Copley, S. D., Frank, E., Kirsch, W. M. & Koch, T. H. Detection and possible origins of aminomalonic acid in protein hydrolysates. *Anal. Biochem.* **201**, 152–157 (1992).

80. Van Buskirk, J. J., Kirsch, W. M., Kleyer, D. L., Barkley, R. M. & Koch, T. H. Aminomalonic acid: identification in Escherichia coli and atherosclerotic plaque. *Proc Natl Acad Sci U S A* **81**, 722–725 (1984).

81. van der Goot, A. T. & Nollen, E. A. A. Tryptophan metabolism: entering the field of aging and age-related pathologies. *Trends Mol Med* **19**, 336–344 (2013).

82. Goot, A. T. van der *et al.* Delaying aging and the aging-associated decline in protein homeostasis by inhibition of tryptophan degradation. *PNAS* **109**, 14912–14917 (2012).

83. Blohmke, C. J. *et al.* Interferon-driven alterations of the host's amino acid metabolism in the pathogenesis of typhoid fever. *J. Exp. Med.* **213**, 1061–1077 (2016).

84. Croitoru-Lamoury, J. *et al.* Interferon-γ regulates the proliferation and differentiation of mesenchymal stem cells via activation of indoleamine 2,3 dioxygenase (IDO). *PLoS ONE* **6**, e14698 (2011).

85. Ichihara, A. Isozyme patterns of branched-chain amino acid transaminase during cellular differentiation and carcinogenesis. *Ann. N. Y. Acad. Sci.* **259**, 347–354 (1975).

86. Lu, G. *et al.* A novel mitochondrial matrix serine/threonine protein phosphatase regulates the mitochondria permeability transition pore and is essential for cellular survival and development. *Genes Dev.* **21**, 784–796 (2007).

87. Gray, S. *et al.* Regulation of gluconeogenesis by Krüppel-like factor 15. *Cell metabolism* **5**, 305–312 (2007).

88. Sun, H. *et al.* Catabolic Defect of Branched-Chain Amino Acids Promotes Heart Failure. *Circulation* **133**, 2038–2049 (2016).

89. Lerin, C. *et al.* Defects in muscle branched-chain amino acid oxidation contribute to impaired lipid metabolism. *Mol Metab* **5**, 926–936 (2016).

90. Newgard, C. B. Interplay between lipids and branched-chain amino acids in development of insulin resistance. *Cell Metab.* **15**, 606–614 (2012).

91. Zhang, Y.-K. *et al.* Enoyl-CoA hydratase-1 regulates mTOR signaling and apoptosis by sensing nutrients. *Nat Commun* **8**, 1–16 (2017).

92. Peroni, D. *et al.* Stem molecular signature of adipose-derived stromal cells. *Exp. Cell Res.* **314**, 603–615 (2008).

93. Pesta, D. & Gnaiger, E. High-resolution respirometry: OXPHOS protocols for human cells and permeabilized fibers from small biopsies of human muscle. *Methods Mol. Biol.* **810**, 25–58 (2012).

94. López-Armada, M. J. *et al.* Mitochondrial activity is modulated by TNFalpha and IL-1beta in normal human chondrocyte cells. *Osteoarthr. Cartil.* **14**, 1011–1022 (2006).

95. Zahn, J. M. *et al.* Transcriptional Profiling of Aging in Human Muscle Reveals a Common Aging Signature. *PLOS Genetics* **2**, e115 (2006).

96. Kriete, A. *et al.* Cell autonomous expression of inflammatory genes in biologically aged fibroblasts associated with elevated NF-kappaB activity. *Immunity & Ageing* **5**, 5 (2008).

97. Puthia, M. *et al.* IRF7 inhibition prevents destructive innate immunity-A target for nonantibiotic therapy of bacterial infections. *Sci Transl Med* **8**, 336ra59 (2016).

98. Wang, X.-A. *et al.* Interferon regulatory factor 7 deficiency prevents diet-induced obesity and insulin resistance. *Am. J. Physiol. Endocrinol. Metab.* **305**, E485-495 (2013).

99. Cheng, Z. & Ristow, M. Mitochondria and Metabolic Homeostasis. *Antioxidants & Redox Signaling* **19**, 240–242 (2013).

100. Taylor, R. C. & Dillin, A. Aging as an Event of Proteostasis Collapse. *Cold Spring Harb Perspect Biol* **3**, a004440 (2011).

101. Chandel, N. S. Evolution of Mitochondria as Signaling Organelles. *Cell Metabolism* **22**, 204–206 (2015).

102. Suhm, T. *et al.* Mitochondrial Translation Efficiency Controls Cytoplasmic Protein Homeostasis. *Cell Metab.* **27**, 1309-1322.e6 (2018).

103. Wrobel, L. *et al.* Mistargeted mitochondrial proteins activate a proteostatic response in the cytosol. *Nature* **524**, 485–488 (2015).

104. Schoggins, J. W. *et al.* A diverse range of gene products are effectors of the type I interferon antiviral response. *Nature* **472**, 481–485 (2011).

105. Nathan, C. & Ding, A. Nonresolving Inflammation. *Cell* **140**, 871–882 (2010).

106. Garaude, J. *et al.* Mitochondrial respiratory-chain adaptations in macrophages contribute to antibacterial host defense. *Nat. Immunol.* **17**, 1037–1045 (2016).

107. Jin, Z., Wei, W., Yang, M., Du, Y. & Wan, Y. Mitochondrial complex I activity suppresses inflammation and enhances bone resorption by shifting macrophage-osteoclast polarization. *Cell Metab.* **20**, 483–498 (2014).

108. Franceschi, C., Garagnani, P., Vitale, G., Capri, M. & Salvioli, S. Inflammaging and 'Garb-aging'. *Trends in Endocrinology & Metabolism* **28**, 199–212 (2017).

109. van Horssen, J., van Schaik, P. & Witte, M. Inflammation and mitochondrial dysfunction: A vicious circle in neurodegenerative disorders? *Neurosci. Lett.* **710**, 132931 (2019).

110. Zhang, Q. *et al.* Circulating mitochondrial DAMPs cause inflammatory responses to injury. *Nature* **464**, 104–107 (2010).

111. Kim, J. *et al.* Mitochondrial DNA damage is involved in apoptosis caused by pro-inflammatory cytokines in human OA chondrocytes. *Osteoarthr. Cartil.* **18**, 424–432 (2010).